Int. Conf. Manufacturing Technology, September (1967), Am. Soc. Tool and Mfg. Engineers.
[25] Langenecker, B., Illiewich, S., and Vodep, O., "Basic and applied research on metal deformation in macrosonic fields at PVL-Austria", Conf. Proc. Ultrasonics Int. (1973) sponsored by J. Ultrasonics.
[26] "New Developments In Metal Working Processes", paper, 83rd Meeting Acous. Soc. Am., Buffalo, New York, 18–21 April 1972, Shoh, A.
[27] Midler, M., United States Patent number 3,510,266 (May 6, 1970).
[28] Klink A., Midler M., and Allegretti J., "A Study of Crystal Cleavage by Sonifier Action", Chemical Engineering Progress Symposium Series, No. 109, 1971, Vol. 67.
[29] "The Silent Treatment", Time Magazine, February 11, 1974, pp. 74–75.

Industrial Applications of Ultrasound—A Review II. Measurements, Tests, and Process Control Using Low-Intensity Ultrasound

LAWRENCE C. LYNNWORTH

Abstract—**The following applications are reviewed: ultrasonic measurement of flow, temperature, density, porosity, pressure, viscosity and other transport properties, level, position, phase, thickness, composition, anisotropy and texture, grain size, stress and strain, elastic properties, bubble, particle and leak detection, nondestructive testing, acoustic emission, imaging and holography, and combinations of these. Principles, techniques, equipment, and application data are summarized for these areas. Most of the measurements utilize approaches designed to respond primarily to sound speed, but some depend on attenuation effects. Most equipment in use involves intrusive probes, but noninvasive, externally-mounted transducers are being promoted in several areas. Both pulse and resonance techniques are widely used. Limitations due to the influence of unwanted variables are identified in some cases. A bibliography and list of vendors provide sources for further information.**

INTRODUCTION

THE MAIN purpose of this review is to identify the breadth, depth, practicality, and limitations of industrial applications of small-signal ultrasound. Additionally, we will attempt to identify patterns of emerging ultrasonic technology.

In general, the scope of this review will be limited to industrial applications wherein the transduction or propagation of low-intensity ultrasound responds to the properties, state, or quality of the medium or prrt in question. By restricting the scope to "industrial" applications we choose to omit numerous interesting and important applications in research, and in medical, dental, and biological areas. "Low-intensity" avoids macrosonic and nonlinear acoustic areas such as ultrasonic cleaning, machining, wire drawing, welding, atomizing cavitating, emulsifying, influencing of chemical reactions shock-wave measurements, and therapy. By limiting the scope to cases where the objective is measuring ultrasound *transduction or propagation* to indicate the value of some variable parameter, we intend to detour around devices such as quartz clocks, ultrasonic garage door openers, TV channel selectors, delay lines, filters, and signal processors despite the obvious industrial significance of such devices. In view of all these omissions, the reader may rightfully ask, "What's left?" For the answer see Table I.

This review generally makes no attempt to identify the earliest demonstration of the entries in Table I, nor to compare with competing technologies. Readers interested in the origins of acoustical measurements of sound speed, attenuation, polarization, or related quantities are referred elsewhere.[1]

Standard commercial equipment, particularized for a specific application, is available for almost every item on the list. Additionally, since virtually any ultrasonic measurement can be analyzed in terms of observations related to transit time or wave amplitude, general-purpose electronic measuring equipment such as digital processing oscilloscopes, computing counters, time intervalometers, peak detectors, etc., may also be used to perform the industrial measurements or tests to be discussed below.

The items in Table I could be categorized into two major groups in terms of instrument response being associated primarily with sound speed c or attenuation coefficient

Manuscript received November 8, 1974.
The author is with Panametrics, Waltham, Mass. 02154.

[1] R. B. Lindsay, ed., *Acoustics—Historical and Philosophical Development* (1973); *Physical Acoustics* (1973), Dowden, Hutchinson and Ross Inc., Stroudsberg, Pa. See also: D. M. Considine, ed., *Encyclopedia of Instrumentation and Control*, McGraw-Hill, New York (1971).

TABLE I
INDUSTRIAL MEASUREMENT, TEST, AND PROCESS CONTROL APPLICATIONS, PARTIAL LIST

Item No.	Parameter
1	Flowmetry
2	Thermometry
3	Density, porosity
4	Pressure
5	Dynamic force, vibration, acceleration
6	Viscosity in fluids
7	Other transport properties
8	Level
9	Location of low-reflectivity interfaces
10	Phase, microstructure, nodularity
11	Thickness
12	Position
13	Composition
14	Anisotropy, texture
15	Nondestructive testing
16	Grain size in metals
17	Stress and strain
18	Acoustic emission
19	Imaging, holography
20	Elastic properties
21	Bubbles and particles
22	Gas leaks
23	Interrupted sound beam
24	Burglar detection
25	Other applications

α.[2] This might be useful academically to individuals who are not necessarily responsible for solving a specific industrial measurement problem. However, if one were to shrink Table I down to these two main groups, without exposing the contents of each group, the present scope of ultrasonic test and measuring equipment would remain obscure. Guidance on the selection of standard equipment for particular applications (flow, temperature, pressure, etc.) would still be lacking. For these reasons, this review is organized in terms of the industrial user's language. Even so, space allows only a small sampling of available ultrasonic equipment to be illustrated.

In the following sections, this review attempts to clarify the listed applications, by introducing the parameter and/or a typical measurement or test situation and then presenting a brief explanation of the measurement or test in terms of the influence of the parameter upon the sound wave's propagation or transduction. Then, rather than elaborate on physical principles and electronic processing of received ultrasonic waves, we choose instead to identify probes or equipment specifically designed to measure the parameters listed. In this way it is intended to clarify the extent to which theory and experiment have been reduced to commercial practice.

At the outset, however, the reader is cautioned that despite the widespread use of a particular product, a full understanding of the wave/parameter interaction and electronic instrumentation details is probably the best insurance against wasting time and money attempting to use standard equipment beyond its inherent limitations, which limitations may be unknown even to the vendor. That is to say, one must strive to understand the relationship between the parameter and c or α. Furthermore, the influence of undesired variables must also be assessed properly.

At the end of this article, references and vendors are grouped corresponding to the item number in Table I.

1. FLOWMETRY

Industrial applications for ultrasonic flowmeters include gas, liquid, and solid matter; flow magnitudes up to a few meters per second for most liquid cases, and potentially even beyond Mach 1 for gases in wind tunnels; conduit sizes from <1 cm diameter to >1 m diameter; rivers, weirs or flumes with open tops; temperature from cryogenic levels (liquid oxygen, liquid natural gas) to potentially at least 1500°C (liquid steel); pressures from near-zero (suction-pumped polymers) to hundreds of atmospheres (pumped oil, deep sea water); response times from a few milliseconds (engine control) to 24 hours (exhaust stack monitoring); single- and two-phase media; etc.

At present, there are approximately 1000 ultrasonic flowmeters in use. Most of these measure water flow in large pipes, $\gtrsim$0.3 m diameter. Almost all of these applications were developed in the last 10 years.

An interesting review of ultrasonic flowmeter development prior to 1957 is due to del Grosso. The earliest reference he found on the use of sound to measure fluid flow in a pipe dated back to Rutten's German patent issued in 1931. Attempts to commercialize on ultrasonic flowmeters in the fifties did not materialize into successful products, whereas now, some 20 years later, a more optimistic situation prevails. The present U. S. A. sales exceed \$1M, and are predicted to exceed \$10M before the end of this decade. Concern with energy transfer, material transfer, process control, and pollution studies will account for much of the predicted market.

Physical Principles

Algebraically, one can summarize the interaction of ultrasound and flow quite easily. For simplicity, if we consider sound waves propagating a distance L axially, upstream and downstream in a pipe, the time difference for the two opposite directions is

$$\Delta t = t_2 - t_1 = 2Lv/c^2 \qquad (1\text{-}1)$$

where v = flow velocity and c = sound speed. In many, but not all cases, the fluid temperature T varies so much that v cannot be calculated to 1% accuracy by (1-1)

[2] In some industrial applications it is required to measure c or α *per se*. Special oceanographic probes and readout equipment have been developed for measuring c vs depth. Backings or isolation members for flaw-detection transducer search units are characterized by α. Delay line materials are partly characterized by both c and α.

unless T is measured accurately, for a well-defined fluid, or, preferably, unless c is measured directly, to avoid errors due to T or composition uncertainties.

On the other hand, if one measures or generates quantities proportional to the reciprocals of t_1 and t_2:

$$\Delta f = f_2 - f_1 = | 1/t_2 - 1/t_1 | = 2v/L \qquad (1\text{-}2)$$

then the c dependence is avoided. As expected, most flowmeters take advantage of this latter equation, using sing-around circuits or servoed-frequency approaches to measure f_1, f_2, and/or Δf.

Still another case is of interest, wherein one measures the Mach number v/c. This ratio, when multiplied by the fluid's characteristic impedance ρc, yields a term proportional to ρv, the mass flow rate. Methods for determining ρc in liquids include crystal impedance measurements and, more recently, reflection coefficient measurements at the end of a wetted buffer rod. Note that v/c can be obtained in several ways: as the ratio $(t_2 - t_1)/(t_2 + t_1)^2$, as the product $c\Delta t$, from the angle of beam drift, and from Doppler measurements.

Other physical principles involved in ultrasonic flowmeters include acoustic noise detection (for flow vs no-flow discrimination), correlation (for measuring travel time of inherent or induced tags or patterns), and ultrasonic pulse-echo level detection (to correct readings in partly-filled conduits, or to obtain readings of flow, in weirs or flumes, wherein level and flow rate are related by a calibration function). Ultrasonic detection of the frequency that vortices are shed off a strut in a flowstream is accomplished in commercially available fluid flowmeters by sensing the modulation which the vortices impose upon ultrasound beamed diametrically across the fluid. It also should be possible in some cases to detect the shedding frequency on the strut itself by alternative ultrasonic means, namely, by applying the acoustic emission principles referred to in Section 18.

The aforementioned equations usually need to be modified somewhat to take into account the angle between the ultrasonic path and the flow axis, to correct for conduit curvature in nonrectilinear conduits, and often most importantly, to convert from a velocity measurement v_d averaged over a single path to the desired area average v_a ($v_a = Kv_d$). Regarding the last item, conversion factors for liquid flow are typically $K = 0.75$ for laminar flow, $K = 0.90$ to 0.96 for turbulent steady flow, and $K = 0.995$ for some turbulent dynamic flow cases.

Flow Cell and Transducer Configurations

Figures 1a–n illustrate present flowmeter cell and transducer designs. Figure 1a shows typical 45° recessed transducer ports, single path; Fig. 1b, screened 45° ports to minimize eddies and improve linearity and a rectilinear flow channel and beam for linear response (area-averaging) independent of profile. Figure 1c shows a 4-chord Gaussian quadrature method for area-averaging, which presently provides the highest accuracy, ~0.1%, at least in pipes large enough to accommodate the 4 paths. Figure 1d is an externally-mounted refraction method using separate wedges; Fig. 1e in effect uses wedges of the same material as the pipe. Figure 1f is applicable to weirs and venturi channels. Figure 1g shows a Doppler arrangement used with liquid metals. A vortex shedder is shown later in Fig. 2h. Other designs are also in use, to control refraction, multiple transits, acoustic "short circuit" around the conduit, or to control other problems.

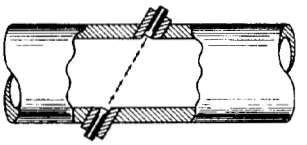

Fig. 1a. Sound bursts are propagated alternately in opposite directions between a pair of transducers situated diagonally along the pipeline. The upstream signal is delayed and the downstream signal is speeded up by the moving fluid. Illustration courtesy Saratoga Systems Inc.

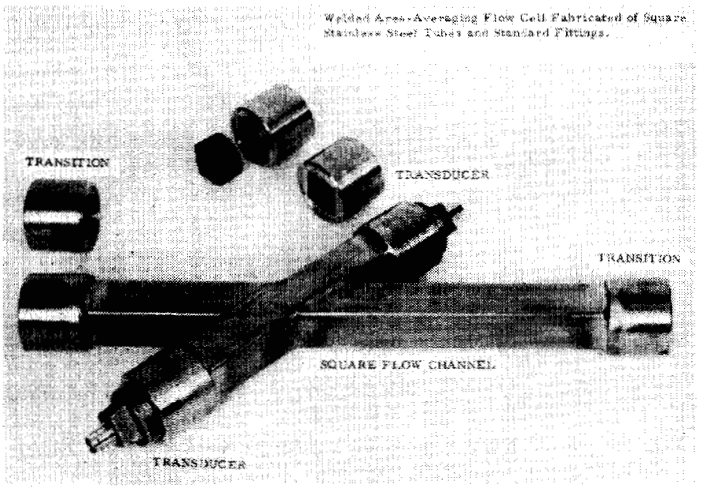

Fig. 1b. Area-averaging flowmeter cell consists of rectilinear flow channel, rectilinear transducer channel, screens over transducer ports to minimize eddy generation therein, and gradual inlet transition. Transducers interrogate 100% of flow channel cross section. This approach provides essentially linear response over laminar, transitional, and turbulent flow regimes.

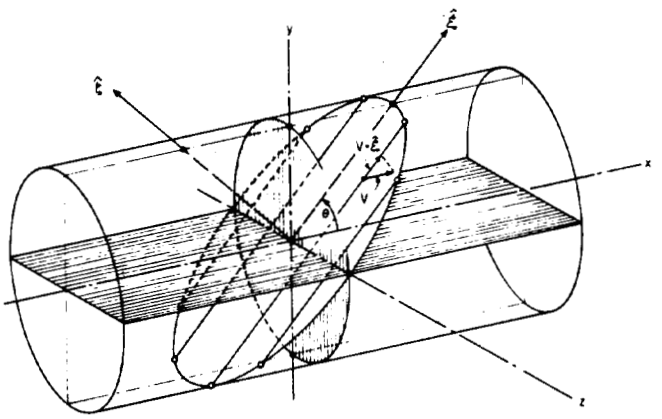

Fig. 1c. Gaussian quadrature flow velocity measurement chords. An ellipse is defined by the intersection of the measurement plane with the pipe wall, and volumetric flow rate is given by the integral of the normal component of the fluid velocity vector $V(z,\xi)$ over the area of the ellipse. After Fisher and Spink (1972).

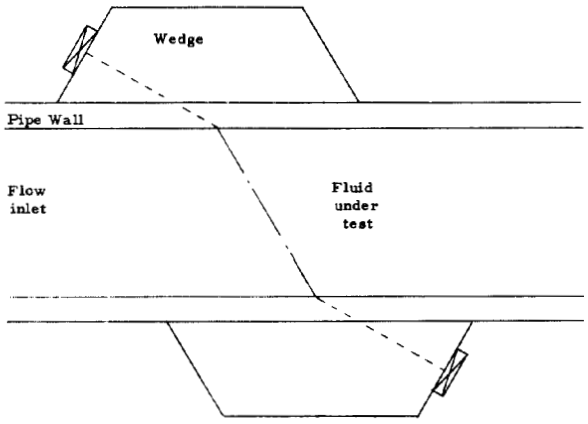

Fig. 1d. Use of externally coupled wedge for introducing longitudinal or shear wave at oblique incidence.

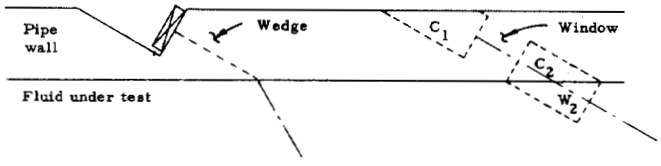

Fig. 1e. (Left) Refracting wedge machined into pipe wall. (Right) Nonrefracting window in pipe wall formed by external cavity C_1 plus internal cavity C_2 or wedge W_2 having parallel faces.

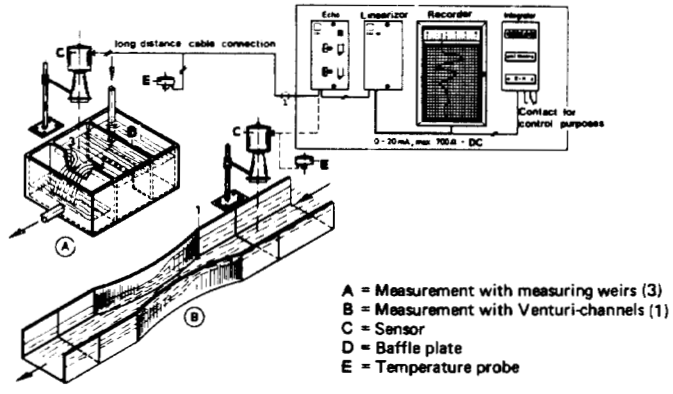

Fig. 1f. Open channel measurements of flow can utilize the reproducible relation between flow and liquid level attending the proper use of a weir, flume, or venturi channel. Noncontact sonic measurement of water level is shown above, where the sensor or transducer C aims a pulse at the surface. The round trip time must be temperature-compensated (see Eq. 2-1). Illustration courtesy Endress & Hauser, Aquatot DMU 160 Manual 6.74.12-0.

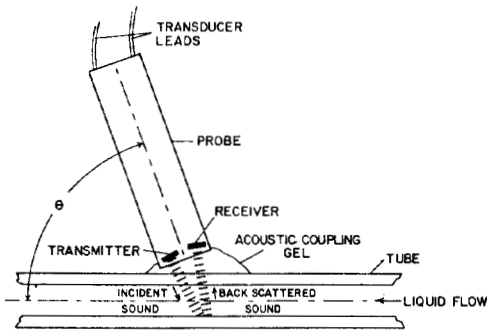

Fig. 1g. Doppler velocimeter for measuring flow, or Mach No. v/c, applied to the liquid metals Hg and NaK flowing in an acrylic tube. Bore diameter was 0.476 cm; transmitted frequency f_0 about 10 MHz; mean flow velocities were about 1 to 5 cm/s. After Fowlis (1973).

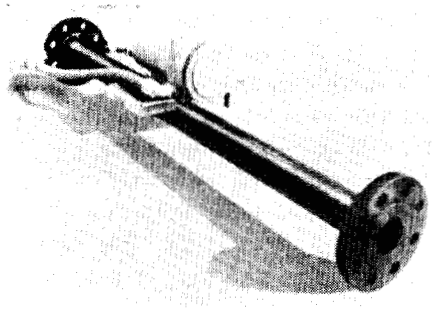

Fig. 1h. Vortex shedding flowmeter. The flowmeter is manufactured in two different models. One is a flow section, 20 diameters in length, as shown above. The other is a "pancake" type, designed for installation between flanges. Pipe diameters range from 1 in. (25 mm) upwards. See also: Ultrasonics 11 (3), 104 (May 1973); Westinghouse Bull. 105-201. Photo courtesy Westinghouse Electric Corp., Computer and Instrumentation Division.

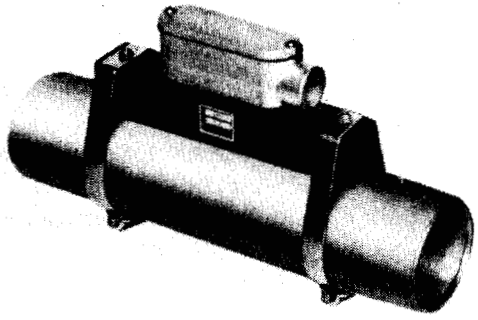

Fig. 1i. Clamp-on flowmeter for pipe diameters of 2.5 cm or larger. Photo courtesy Controlotron Corp.

Standard clamp-on flowmeters are available commercially for small pipes (diameter $\gtrsim$ 2.5 cm) and large pipes (diameter $\gtrsim$ 30 cm). Clamping pressure is developed by tightening conventional hose clamps or turnbuckles. To obtain reproducible position and orientation of the coupling blocks or wedges, the author utilized sets of bolts whose heads were contoured and then welded to a 7.5 cm diameter tube at jig-controlled coordinates. The bolts then acted similarly to alignment pins, and further, enabled the wedges to be tightened against the tube in a torque-controlled manner. Examples of these clamp-on flowmeters are shown in Figs. 1i, j, k.

The noncontact utilization of magnetostrictive (or electromagnetic) transduction of extensional guided waves to measure the drawing speed of metal wire was suggested by the author (1974). A different noncontact configuration, using electrostatic transducers air-coupled to moving sheets of paper or metal, is under investigation by Luukkala of the University of Helsinki as part of a potential flowmetering system based on guided wave measurements with plate waves.

In contrast to these noninvasive or even noncontact transducer mounts, it is interesting to note that the long-abandoned in-the-flow transducer concept may be re-

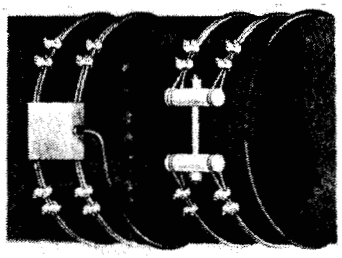

Fig. 1j. Clamp-on flowmeter for pipe diameters larger than 30 cm (1 ft). Illustration courtesy Badger Meter Co.

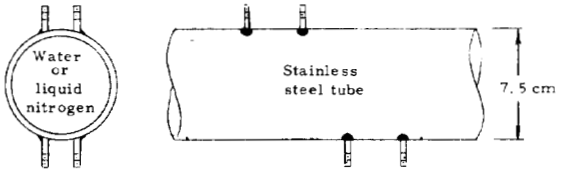

Fig. 1k. Use of welded bolts to position, align, and secure clamp-on transducer wedges (author, 1974).

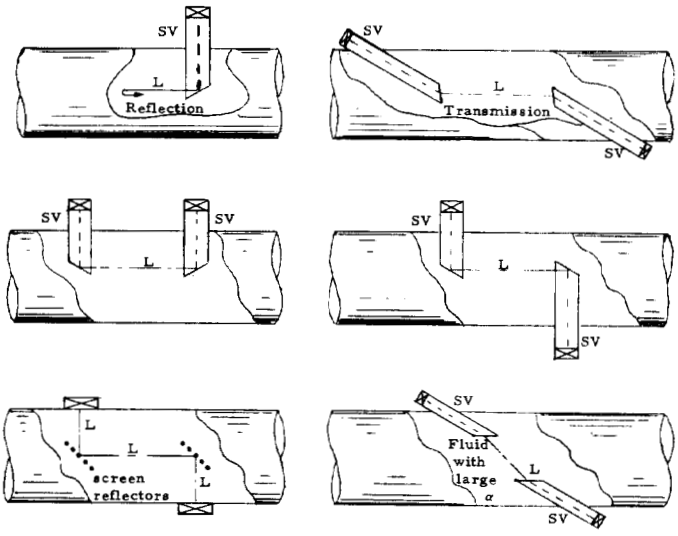

Fig. 1m. Intrusive flowmeter probes with external transducers (Lynnworth, 1967, 1969, 1974).

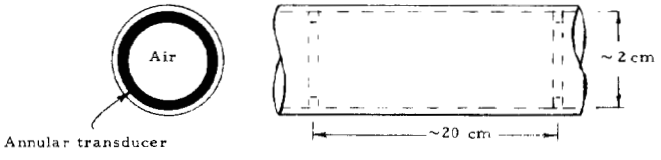

Fig. 1l. Use of intrusive transducers to beam the interrogating waves essentially along axial path. After Frankenberger *et al.* (1974).

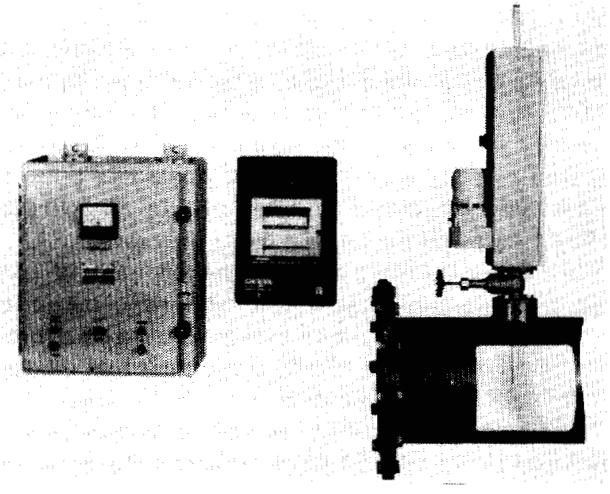

Fig. 1n. Doppler flowmeter probe containing two transducers positioned near axis of pipe. Photo courtesy EDO Corp.

vitalized for specific applications. The motivation is to trade nonintrusiveness for axial propagation. Frankenberger *et al.* (1974) concentrically mounted two ~1 MHz pulsed PZT annular transducers within a flow cell tube, to measure laminar air flow (Fig. 1l). The use of a relatively small flow cell, inserted as a probe to scan or to measure flow at a fixed radial distance, has also been suggested (Lynnworth, 1972, 1975). The preferred location for such an invasive probe is where the local v equals the area-averaged v. This occurs at a radius $r = 0.707a$ in a circular duct of diameter $2a$ for laminar (parabolic profile) flow. Area averaging radial distances would be preferred locations for vortex shedding toroids or struts. Again, if these shedders were electroacoustically transductive by virtue of being fabricated at least in part of a piezoelectric or magnetostrictive material, the vibration at the shedding frequency could in some cases, be detected right on the shedder.

Two other intrusive flowmeter probes may be mentioned. The former probe type, Fig. 1m, in most instances is essentially a long buffer rod, beveled or chamfered at one end, designed to penetrate into a fluid whose temperature, corrosiveness, or other attributes provides an intolerable environment for transducers. Shear waves generated at the external transducer, and polarized with a particle displacement component parallel to the flow direction (SV), propagate to the chamfer, where they are mode converted and transmitted into the fluid as longitudinal (L) waves. Part of the L-wave energy refracts, emerging from the chamfer nearly perpendicular to the chamfer. Another part of the L-wave energy reflects internally off the chamfer, emerging from the side of the probe adjacent to the chamfered end, either substantially or in preferred cases precisely perpendicular to the major axis of the buffer rod. Either of these emerging waves can be used to measure flow, utilizing transmission or reflection (Doppler) principles (Lynnworth, 1967, 1969).

The latter intrusive probe type to be mentioned here, Fig. 1n, was introduced by EDO in 1974. It is used in what appears to be the only Doppler industrial flowmeter commercially available at this time for measuring fluid flow in pipes. Transmitting typically near 3 MHz, it uses two transducers aimed at a point 30 cm upstream, in a selectably representative region of flow. That is to say, the probe penetration is adjustable, so one can profile the flow and then position the probe optimally. For example, in some cases the preferred location may be near $r = 0.2a$ for turbulent flow in a pipe of radius a. The dual-trans-

ducer Doppler-probes are dimensioned about 2 cm diameter for pipes up to 60 cm diameter, and 5 cm diameter for pipes up to about 2.5 m diameter. The probes can be cleaned by a wiper assembly on a timed automatic cycle, a useful feature in sewage applications presently under evaluation.

2. THERMOMETRY

Ultrasonic thermometers are usually designed to respond to the temperature-dependence of sound speed c. In special cases where only one particular temperature is of interest, such as the temperature of a phase change, or the recrystallization temperature, the temperature-dependence of attenuation may be utilized.

Ultrasonic thermometers have found applications in the temperature range -80 to $+250$°C, where the "quartz thermometer" offers resolution of 0.1 millidegree and linearity superior to platinum resistance thermometers. Fluidic thermometers, usually oscillating below 10 kHz, are used in quantities over 1000 for aircraft, aerospace, and other engine applications. Sensor temperatures up to 1200°C are fairly common; materials limitations have kept applications up to 2200°C in the short-life, experimental stage.[3] At much higher temperatures, approaching 3000°C, thin-wire probe-type sensors offer accuracy and/or longevity advantages over thermocouples. In studies of the transport properties of gases, ultrasonic pulse techniques have measured temperature in the 10 000 to 20 000°C range, using the gas as its own sensor.

The number of quartz thermometers sold to date is approximately 1600. About 30 thin-wire thermometer probes, and about a dozen corresponding instruments, have been sold to date, chiefly for nuclear fuel pin centerline temperature applications.

Most applications for the preceding devices have been developed in the past 10 years, although the origin of the techniques themselves can be traced to earlier decades. The thin-wire technique, for example, is traceable historically to Bell's pioneering work (1957), and in some respects, to Frederick's notched bar thesis (1947). Quartz crystal studies date back to the Curie brothers' discovery of piezoelectricity in 1880, but the linear coefficient (LC) cut underlying the quartz thermometer is of more recent vintage (1964).

Physical Principles

The temperature-dependence of c may be computed for gases:

$$c = (\gamma RT/M)^{1/2} \qquad (2\text{-}1)$$

where γ = specific heat ratio C_p/C_v, R = gas constant, T = absolute temperature, and M = average molecular weight. Uncertainties in composition, e.g., incompletely-burned fuel entering a turbine section of a jet engine, place one limit on the ultimate accuracy attainable. Impedance mismatch, attenuation in low-density and/or turbulent gases, and ambient noise place other limits in potential applications where the use of (2-1) has been proposed.

For liquids and solids, the temperature-dependence of c may also be computed, but only in cases where the appropriate modulus and density have been measured previously. The temperature-dependence of c is illustrated in Fig. 2a.

Two basic measurement principles have been used in instruments responding to c: resonance and pulse (nonresonance). The quartz thermometer senses temperature T by the change in resonant frequency of a small quartz disk, ~28 MHz ± 1000 Hz per °C. Fluidic devices oscillate at a frequency determined by sensor geometry and c of the gas passing through the device. Bell's resonant probe may be described as a small tuning fork, whose frequency changes with elasticity and density changes. Bell previously introduced nonresonant thin-wire T-sensing probes, which were subsequently developed by Bell's co-workers, particularly Thorne, and later, by this author and his colleagues, and also by other investigators. A hybrid technique wherein a broad-band pulse impulsively drives a short sensor into resonance was developed by Fowler. Using pulse techniques, dual- and multi-zone profile thin-wire sensors were demonstrated by this author and right angle wire sensors by Fam.

Equipment

Ultrasonic thermometry applications have been reviewed in recent IEEE and ISA symposia proceedings. Let us not reiterate their contents, but rather, let us now proceed to illustrate examples of available equipment. Figure 2b shows the Hewlett-Packard quartz thermometer; Fig. 2c, a fluidic thermometer; Fig. 2d, resonator probes; Fig. 2e, a nonresonant single-zone wire sensor; and Fig. 2f, nonresonant multizone wire sensors. Figure 2g illustrates the concept of profiling the temperature inside a solid body, such as a steel billet. Figure 2h illustrates a noninvasive measurement of a fluid within a conduit, such as liquid sodium in a stainless steel pipe.

3. DENSITY, POROSITY

Some ultrasonic measurements of density ρ and porosity q may initially appear analogous to well-known gamma-ray measurements based on backscatter or on absorption principles. However, the ultrasonic energy/matter interaction is quite different from that for gamma rays. The differences may be clarified with reference to the following applications of ρ measurement in gases and liquids, and ρ and q measurements in solids.

We consider several probe-type resonant and nonresonant densitometers, which are ordinarily immersed partly or totally in the fluid under test, and also nonpenetrating transmission-type devices or measurements wherein c or α is a function of ρ or q. The former type

[3] Fluidic devices, despite their oscillations usually occurring below the ultrasonic range, are included in this section only because their response to temperature follows (2-1). However, their use relative to many other industrial parameters such as position, pressure, etc., is not discussed in this review.

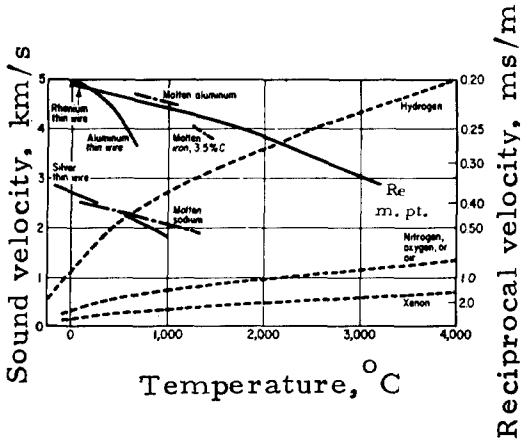

Fig. 2a. Ultrasonic velocity in several materials as a function of temperature.

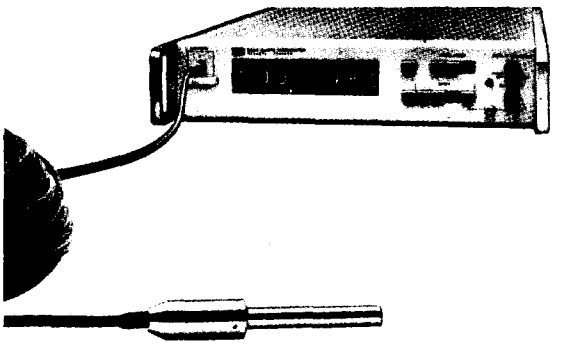

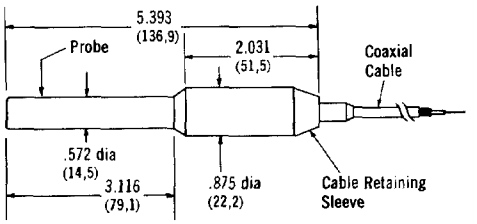

Fig. 2b. Quartz thermometer, HP 2801A, and oceanographic temperature sensor assembly 2833B with outline dimensions in inches and (mm). This probe operates from −40 to +120°C, and is rated for 10 000 psi (equivalent to ocean depth of over 4 miles, or nearly 7 km). Nominal operating frequency is 28 MHz; sensitivity to temperature change is approximately 1000 Hz per °C.

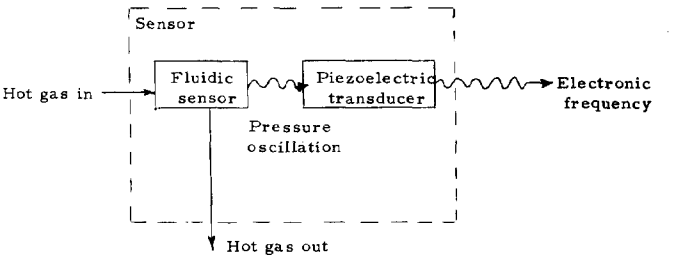

Fig. 2c. Fluidic thermometer element and transducer, operational schematic, after McMillan and Pamperin (1972).

No.	Resonator	Q	Diameter ratio for Q = 50	Features
1	λ/2	π/2r	0.125	Can be supported at centre which is a node. Requires a high temperature junction.
2	λ/4	π/4r	0.087	Can be made an integral part of the line by chemical machining.
3	λ/4 λ/4	$\pi/2r^2$	0.421	Requires a minimum machining for given Q. Is integral with line.
4	λ/4 λ/4	$\pi/4r^2$	0.353	Can be supported on large diameter section.
5		Not readily analysed		Flexure "tuning fork" mode. Identical calibration of batch. Shape inconvenient.

Fig. 2d. Shapes and characteristics of resonant thermometer sensors, after Bell (1972).

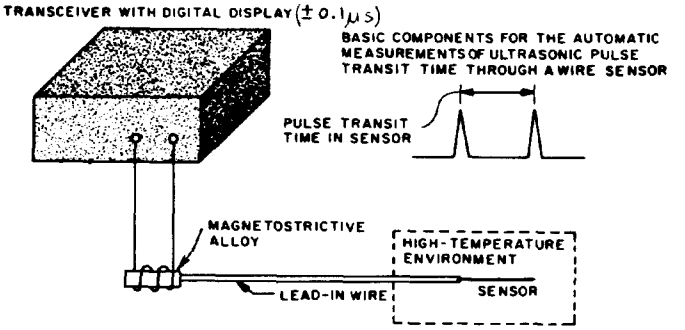

Fig. 2e. Temperature sensing probe, with single-zone sensor being nonresonant.

may be understood by analyzing sound propagation in the probe (which is "loaded" by the fluid). The latter type is understood by analyzing propagation in the fluid or solid medium itself.

Resonant Probe Principles

The ITT Barton densitometer probe, Fig. 3a, consists of a sensing vane symmetrically positioned across a supporting cylinder. In operation, the vane oscillates to move with a simple harmonic motion, causing an acceleration of the surrounding fluid.

The vane oscillates at a resonant frequency determined by the density of the surrounding fluid. As the fluid density increases, the frequency of vibration decreases. Similarly, as the density decreases, the frequency of vibration increases in accordance with the following general relationship:

$$\rho = A/f^2 + C \qquad (3\text{-}1)$$

where A and C are constants and f = frequency.

The probe is installed in a line containing fluid. A detector within the probe senses the frequency of the vibrating vane. This signal is amplified in the transmitter and energizes a driver within the probe with a minimum force to sustain oscillation at the system resonant frequency.

Probes can operate with fluids in static or dynamic situations, and from cryogenic to over 100°C. Precision is 0.1% of full scale. Applications include aerospace,

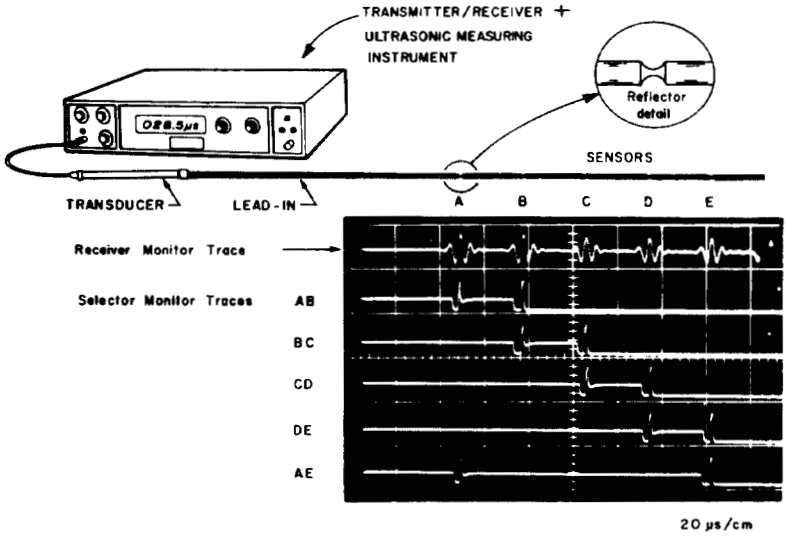

Schematic and oscillogram illustrate ultrasonic temperature profiling. Single line containing series sensors is scanned by selecting echoes according to sensor position along the line. Transit time (microsecond) between selected pair of echoes corresponds to temperature between reflection points. Echo pairs AB, BC, CD, DE yield profile; pair AE yields average temperature.

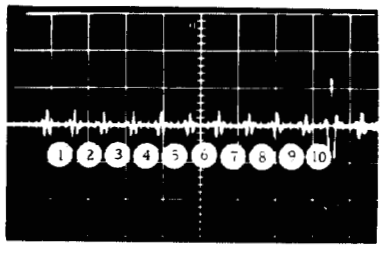

Oscillogram shows echoes reflected from the ends of ten temperature sensors connected in series on one single wire line.

Fig. 2f. Multizone temperature sensors.

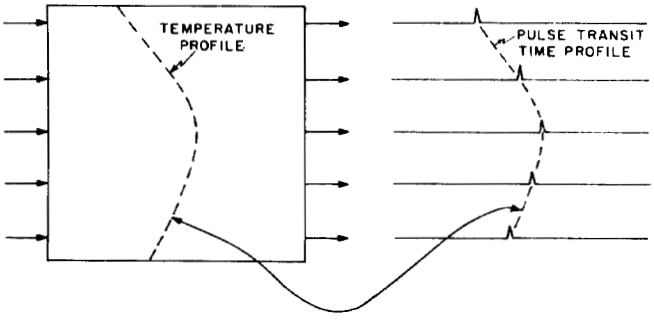

Fig. 2g. Ultrasonic determination of temperature distribution inside large metal billets.

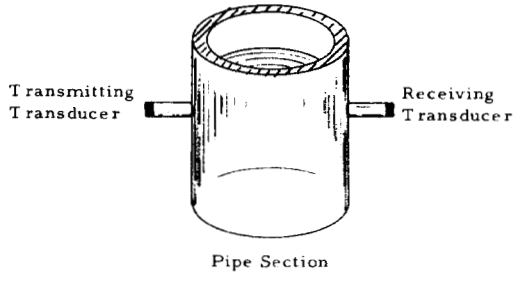

Fig. 2h. Temperature of liquid sodium was determined by measuring transit time of ultrasonic pulse transmitted across the diameter (25 cm). Probes were noninvasive. They were removed after test. Test site: Argonne National Laboratory, oscillator rod facility, May 1968.

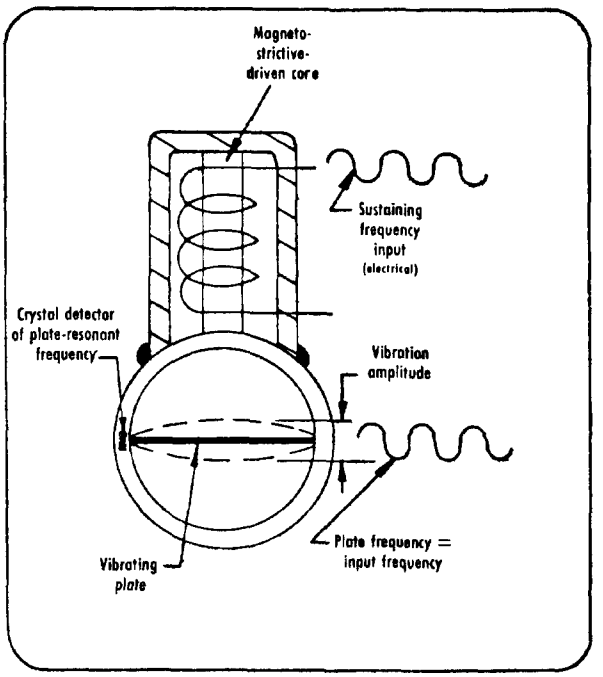

Fig. 3a. ITT-Barton vibrating plate densitometer, showing magnetostrictive driver and piezoelectric detector. After November (1972).

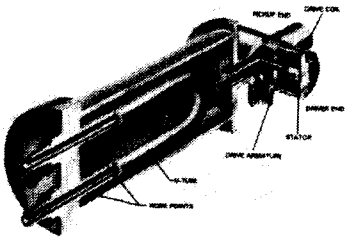

Fig. 3b. Dynatrol® U-tube resonator measures density/specific gravity/% solid concentration. Illustration: Automation Products, Inc.

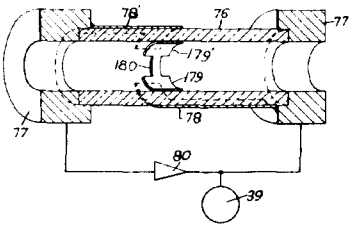

Fig. 3c. Densitometer probe consisting of hollow piezoelectric cylinder. After Abbotts (1972).

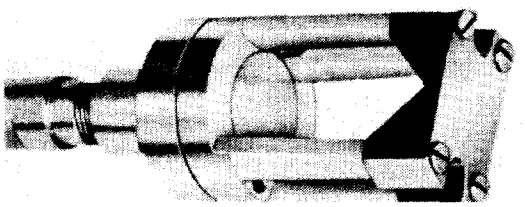

Fig. 3d. Sound velocity probe consisting of transducers and a corner reflector, and normally used for composition and interface measurements, can be used in some cases to determine liquid density. Illustration courtesy NUSonics, Inc.

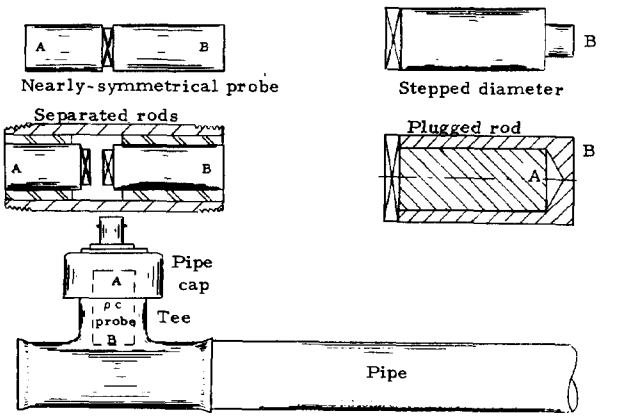

Fig. 3e. Example of ρc densitometer probes, and one view of a ρc probe potted within a standard pipe tee.

chemical, petrochemical, refineries, pipelines, cryogenic, and food processing. Liquid applications are limited to viscosities less than ~100 centipoise. Some 300 densitometers of this type have been sold since it was introduced in 1971.

Another resonant probe design, Fig. 3b, is available from Automation Products. Here, liquid (even of very high viscosity) passes through a U-tube, and the resonant frequency of the filled tube indicates ρ.

Hoop-mode vibrations are utilized in fluid densitometers available from Fluid Data, Inc., and from Solartron/Rockwell Manufacturing Company (e.g., Abbotts, 1972, see Fig. 3c). (Both the vane and U-tube probes normally resonate in the audible, not ultrasonic, range. Nevertheless, their inclusion in this review is considered justified by their physical principles.)

Since about 1955, several investigators have considered measuring the electrical impedance of a crystal radiating into a liquid, to determine the liquid's characteristic impedance ρc. This approach apparently has not yet proven practical.

Relative to an orbiting densitometer, gases at densities as low as air at 140 to 280 km have been tested with a resonant quartz crystal used as a microbalance. Response was reported as linear for pressures from 10^{-4} to 2×10^{-6} Torr, with sensitivity of 1.7×10^{8} Hz/g, and accuracy of 6% (see Roder, 1974).

Nonresonant Probe Principles

A pulse-echo sound velocity probe, Fig. 3d, developed by NUSonics primarily for applications described in Sections 9 and 13 can also be used for ρ determinations in cases where ρ is a known function of c. Probes may be mounted recessed or in-stream. In either case the measurement is based on propagating a pulse between the transducer and the reflector, over a defined liquid path.

Another pulse-echo probe, Fig. 3e, is under development at the author's laboratory, to measure ρc of liquids. This reflection probe offers potential advantages over those shown in Figs. 3a–d, in that it is small and flush-mounted, its installation producing essentially no pressure drop or

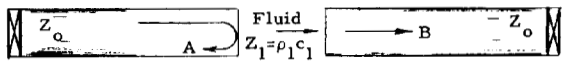

Fig. 3f. Transmission measurement of fluid properties, using buffer rods.

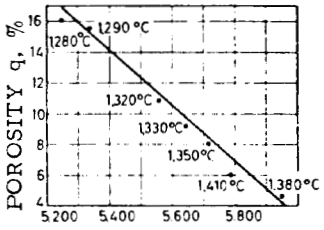

Fig. 3g. Variation of absolute porosity versus longitudinal wave velocity for one type of electrically insulating porcelain, after Filipczynski *et al.*, p. 255 (1966).

disruption of the flow. Ultimately, this approach is amenable to external mounting. Its fundamental limit is that ρc is sensed in the rather thin layer of liquid adjacent to the wetted portion of the probe. Thus, buildup of deposits would prevent an accurate measure of the free-stream liquid. The ρc probe may be combined with an independent measurement of c, to yield ρ, or combined with a measurement of v/c, to yield mass flow rate, e.g., mass flow rate of fuels. This reflection coefficient concept may also be applied to determining ρ of solids, but not gases.

Transmission Principles

Gas Density: The relative amplitude of a received pulse, after transmission across a *gas* (Fig. 3f) depends mainly on the impedance mismatch at the buffer rod/gas interfaces, and on the attenuation losses in the gas. For the symmetrical case illustrated, and neglecting beam spread, it may be shown that, in terms of the reference echo amplitude A, and the first and second amplitudes B and C corresponding to single and triple transmissions across the gas path L, the gas density ρ_1 is given by

$$\rho_1 = (Z_0/4c_1) \mid B/A \mid (B/C)^{1/2} \qquad (3\text{-}2)$$

where c_1 = sound speed in the gas and Z_0 = buffer rod characteristic impedance. (Mismatch and attenuation losses may be separated alternatively by using two different paths L_1 and L_2, or by transmitting two different frequencies, since $\alpha \sim f^2$, but mismatch losses are independent of f, when dispersion is absent.)

In gas volumes containing temperature gradients, there exist ρ gradients even though pressures may be substantially uniform. Measuring the ρ distribution is important, for example, in aerodynamic tests in ducts where total gas mass flow rate is to be computed as the area integral of local ρv products. One noninvasive ultrasonic approach to this problem is to measure the c distribution by the transmission methods of Section 2. Now, if the c distribution can be translated to a T distribution (see Fig. 2h), and if p is known at one location, say, at the inside wall of the duct, then in principle T and p can be combined to yield ρ as a function of duct coordinates. In effect, this exploits the expression for c in an ideal gas, $c = (\gamma p/\rho)^{1/2}$.

Liquid Density: For liquids which can be interrogated as in Fig. 3f at a frequency where αL is very small compared to mismatch losses, the density is given by

$$\rho_1 = (Z_0/c_1) \mid B/4A \mid \qquad (3\text{-}3)$$

where the subscript 1 now refers to the liquid.

On the other hand, in slurries, sludge, or similar two-phase media, αL may be very large compared to mismatch losses. In some such cases the fluid density may be empirically correlated with attenuation.

A noninvasive alternative to Fig. 3d may also be considered, in some cases. That is to say, externally mounted transducers may be arranged to measure c within a conduit, for situations where ρ is a known function of c. See also, Section 21 and Fig. 2h.

Solid Density: The density of a solid member, at least one surface of which is immersed in a liquid such as water, can be measured by reflection coefficient principles. This application is the dual of that indicated in Fig. 3e.

The density of solid sheets of known thickness l very thin compared to wavelength λ may be determined based on reflection and transmission coefficient principles. Density is computed using an approximation of the form

$$\rho = AZ_0/\pi Bfl \qquad (3\text{-}4)$$

where A and B are amplitudes of reflected and transmitted rf bursts of center frequency f, and Z_0 = characteristic impedance of the medium on both sides of the sheet.

Porosity: Analogous to liquid densitometry based on proportionality or correlation of ρ and c, useful determinations of porosity q in some ceramics, particularly porcelain, have been obtained from c measurements. See Fig. 3g. In relation to dielectric properties of porcelain insulators, Filipczynski *et al.* (1966) reported that optimum sintering occurs at the maximum wave velocity corresponding to minimum porosity (example: 1380°C firing temperature). Within limits, porosity is reduced by higher firing temperatures, the effective wave path being reduced as gas inclusions are filled in by melting. However, too high a temperature (1410°C) causes outgassing, creating new pores, and reducing c. To avoid the q ambiguity, one would follow c during the firing process, or one limits the furnace temperature.

Spriggs (1962) proposed exponential equations of the form $E = E_0^{-b_o q_o - b_c q_c}$ (where E = modulus of porous material, E_0 = modulus of pore-free matrix, b_o and b_c are empirical constants, and q_o, q_c are volume fractions of open and closed pores) to fit elastic moduli data vs porosity. This attempts to take into account open and closed pores, for low porosities, e.g., q up to $\sim$0.16 for cold-pressed and sintered alumina (q = void volume/total specimen volume). Martin and Haynes (1971) proposed an equation of the form $E = E_0 - k_2 E_0 q^{2/3}$ where k_2 = empirical constant depending on average void properties. This expression appears valid for a wide range of porous solids, for q up to a "critical porosity" where $E \lesssim 10\% E_0$.

Hasselman (1962), considering the voids as a dispersed phase within a continuous phase matrix, proposed an equation for the porous composite of the form:

$$E = E_0\left[1 + \frac{bq}{1 - (b+1)q}\right] \qquad (3\text{-}5)$$

but pointed out that in many cases, an increase in q would be accompanied by a change in microstructure or type of porosity. The q-dependence of elastic properties such as E, G, or σ cannot then be expressed by one single equation valid for $0 < q < 1$.

Correlation of reflectance and porosity of sea floor sediment has been studied by several investigators since at least 1965, when Breslau measured ocean bottom returns in the Atlantic, at 12 kHz. See for example, studies by Faas (1969) and subsequent discussions (1971). Correlation coefficients cited in these porosity/reflectance studies range from 0.706 to 0.97.

4. PRESSURE

Pressure influences sound propagation in solids, liquids, and gases, but in different ways. In solids, applied pressure leads to so-called stress-induced anisotropy, as shown by Crecraft, Hsu, and others. See Section 17. In liquids, the effects of pressure p upon c and α are usually small (relative to effects in gases) but the frequency of relaxation peaks can be shifted significantly. However, as students of sonar know, sound speed in the sea increases significantly with depth D due to hydrostatic pressure. The depth coefficient (pressure effect) is $\Delta c/\Delta D = 0.017$ m/(sec)(m); $(\Delta c/c)/\Delta D = 1.1 \times 10^{-5}$/m. In nonideal gases, c increases as p increases, while α is inversely proportional to p. For a nonideal gas, the equation of state may be written $pV = RT + Bp$, where V = volume and B = second virial coefficient. From this,

$$c = (\gamma(RT + 2Bp)/M)^{1/2}. \qquad (4\text{-}1)$$

Standard ultrasonic equipment for measuring p includes a Hewlett-Packard instrument, utilizing another special cut in quartz, and a Wallace and Tiernan sonar manometer. In the former device, Fig. 4a, the quartz crystal responds almost linearly to p, but requires temperature compensation. The probe assembly contains the quartz crystal p-sensing oscillator and a reference oscillator. The p-dependent difference frequency is transmitted up the cable to the signal processor. The p-sensing oscillator typically varies from ~0.5 to ~1 MHz. Range of the quartz pressure gage is 0 to 844 kg/cm² (0 to 12 000 psia), 0°C to 150°C, and resolution is <0.7 g/cm² (0.01 psi) at a 1 second sampling period. Introduced in 1971, about 50 have been sold so far. Field uses include: oil well logging, oceanographic research, pulse tests in wells, and monitoring underground detonations.

In the latter device, Fig. 4b, ultrasonic pulses measure the relative heights of two mercury columns. One piezoelectric transducer mounted at the bottom of each leg of the manometer transmits an ultrasonic pulse through the mercury to the surface and receives the echo from that surface. By transmitting the ultrasonic pulse simultaneously in both legs, the difference in time between reception of the echoes of the two legs can be related to the height difference.

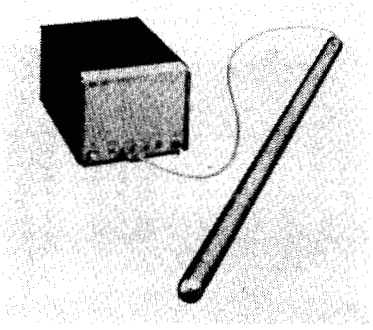

Fig. 4a. Model 2811A quartz pressure gauge uses a unique transducer of a highly stable quartz crystal resonator whose frequency changes directly with applied pressure. Photo courtesy Hewlett-Packard.

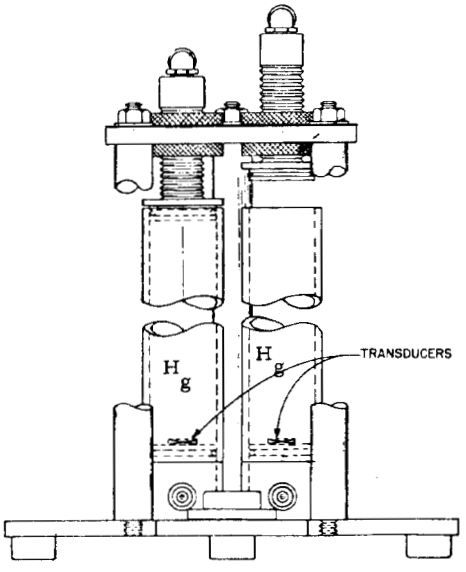

Fig. 4b. In digital U-tube sonar manometer, ultrasonic pulses are used to measure the difference in heights of two columns of mercury. Illustration courtesy Wallace & Tiernan Div., Pennwalt Corp.

By holding c constant, one can relate the time difference to a height difference. A time reference (master-clock oscillator), can be chosen to yield different calibration units. In. Hg, psi, mm Hg, mb, psf, N/m², and Pascals are the standard units available.

Essentially, the return of the first echo (the short leg or column) starts a counter totalizing the clock oscillator cycles. The return of the longer leg or column echo stops the counter. The number of cycles totalled represents the height difference.

Maintaining a constant speed of sound and constant mercury density requires careful temperature control. A mercury-in-glass thermostat is the thermal reference. Control is better than ±0.05°F for accuracy to ±0.0005 in. Hg at 32 in. Hg.

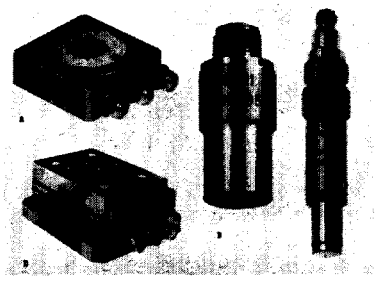

Fig. 5a. Piezoelectric instrumentation includes two- and three-component force-measuring quartz transducers, multicomponent force-measuring dynamometers, high-temperature pressure transducers, and engine pressure gauges for measuring pressure, force, acceleration, torque, cutting forces, etc. Photo credit, Kristal Instruments.

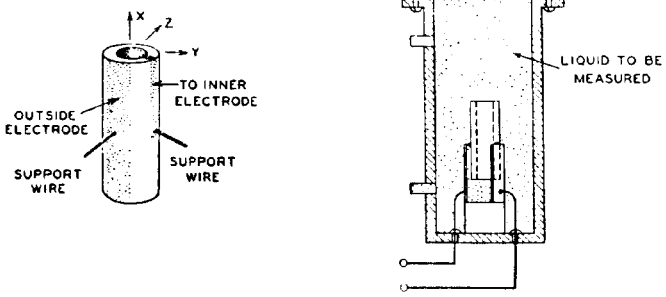

Fig. 6a. Experimental arrangement for measuring η in light liquids, using a torsional transducer, after Mason (1947). The torsional ADP crystal, as shown at the left, is nodally suspended by three wires, and immersed in the liquid under test.

Range of the sonar manometer is 0 to 0.8 m (0 to 32 inch) Hg, resolution is essentially 10 ppm, and calibration accuracy is stated as better than 0.001 inch. Introduced in 1969, some 75 have been sold to date. Applications include calibration of pressure transducers, continuous measurement of pressures in wind tunnels, engine test stands and vacuum chambers, and a barometer for automatic weather stations. In summary, it is used for gauge, absolute or differential pressure, or vacuum.

5. DYNAMIC FORCE, VIBRATION, ACCELERATION

Piezoelectric transducers have been widely used for many years to measure force, vibration, acceleration, torque, etc. Such applications are to be expected from the very definition of a piezoelectric material. In this section we wish to merely note that quartz and other materials are now used in applications from cryogenic to ~800°C, in nuclear environments, up to at least 100 kHz, and provide up to 3 axes of component resolution in packaged units. Application details are readily available from a number of vendors. See Fig. 5a.

6. VISCOSITY IN FLUIDS

According to classical theory, sound absorption in gases is due to the sum of viscous and thermal conduction effects. The α ratio due to these effects lies between about 1 and 3, for common gases:

$$\alpha_{\text{vis}}/\alpha_{\text{th}} = 4\eta C_v\gamma/3K(\gamma - 1) \qquad (6\text{-}1)$$

where η = coefficient of viscosity, C_v = specific heat at constant volume, γ = specific heat ratio, and K = coefficient of thermal conductivity, which equals $2.5C_p\eta/\gamma$ for monatomic gases. Experiments have established that classical theory accounts for absorption in monatomic gases without ionization. In diatomic and polyatomic gases, in binary mixtures, and in reacting gases, attenuation is observed to be higher than the classically predicted value, due to diffusion, relaxation, or internal effects. During the sixties, Carnevale, the author, and co-workers reported on η determinations in argon to ~10^4°K, where η was calculated from the measured attenuation coefficient α:

$$\eta = \alpha\gamma cp/2\pi^2f^2[(4/3) + 5(\gamma - 1)/2\gamma]. \qquad (6\text{-}2)$$

In nonmetallic liquids the classical absorption is essentially due to η since K effects are negligibly small in comparison. Excess attenuation is observed in nonmonatomic liquids, which, as for some gases, can dwarf the classical effects. See, for example, Herzfeld and Litovitz's well-known book (1959). Noninvasive monitoring of viscosity changes characteristic of one polymerization process was demonstrated by this author (1971). The attenuation of pulses transmitted across the 75 mm diameter of stainless steel pipes containing liquids having viscosities of ~50 and ~10^4 centipoise, clearly indicated these large differences in viscosity. But reproducible resolution of small differences in η is another matter.

Presently available equipment for η measurements is not based on the above transmission concepts, but rather, on the damping effects of viscous liquids upon an immersed probe.

Viscosity Probes for Liquids

Ultrasonic η probes utilize several different geometries. Figure 6a shows an immersed torsional wave piezoelectric transducer (Mason, 1947), with which η was measured from 0.01 to 6 poises. Liquids of higher viscosity exhibit a shear stiffness, complicating the analysis of the measured crystal resonance frequency and resistance. Mason *et al.* (1949) also utilized shear wave reflectance at oblique incidence (Fig. 6b). More recently, shear wave reflectance at normal incidence (Fig. 6c) as reviewed by Moore and McSkimin (1970), has been used.

In the Bendix viscometer, for which a variety of metal probes are available, the sensor generally consists of a protected resonant blade including a magnetostrictive portion at one end, and stainless steel at the other. This instrument was introduced in December of 1968, and some 150 were sold by the end of 1974. It operates as follows. (See Fig. 6d, and Frederick, pp. 219, 220.)

Operationally, the probe is inserted into the liquid and the degree of "shearing" or "viscous drag" is translated electronically into a value of viscosity for that particular

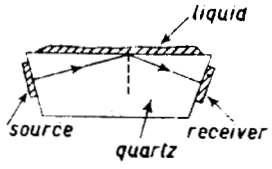

Fig. 6b. Arrangement for production of shear waves in a liquid, after Mason *et al.* (1949).

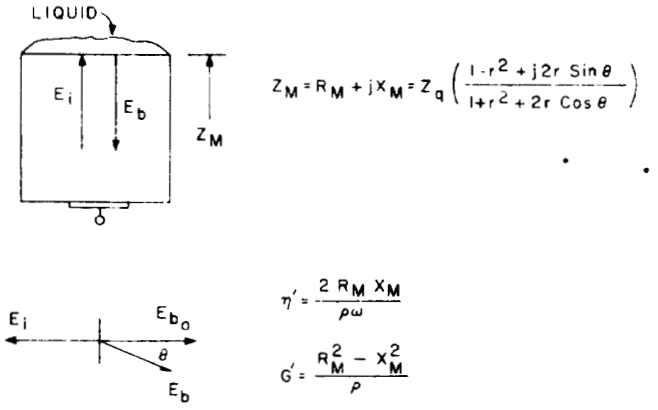

Fig 6c. Basis of shear reflectance method, after Moore and McSkimin (1970).

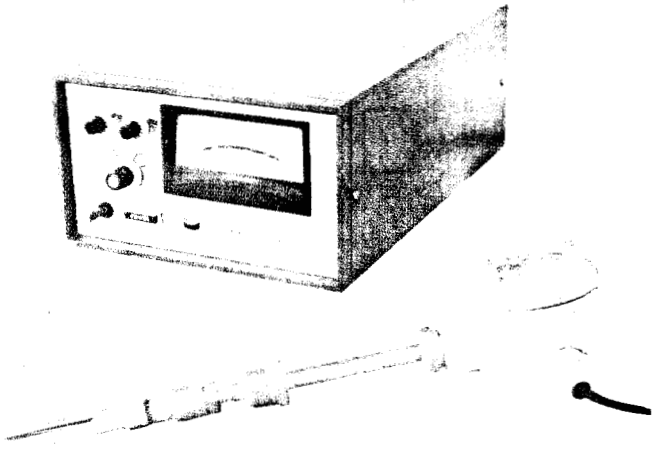

Fig. 6d. Ultra-Viscoson model 1800 viscometer senses damping effect on resonant probe, thereby determining viscosity × density product $\eta\rho$. Photo courtesy Bendix Corp., Process Instruments Div.

liquid, for $\eta\rho$ values ranging in 4 scales up to 50 000 cp × g/cm³. Probes are available to accommodate numerous different liquids at temperature ranges up to +200°C and a pressure range from 0 to 750 psig.

If desired, a number of probes can be connected via a multipoint unit to a single electronic subassembly. This configuration permits measurements of several liquids at a central location.

The electronic subassembly produces a short pulse of current to a coil situated inside the probe and around the thin blade sensing element. The resulting magnetic field excites the magnetostrictive member and causes the blade

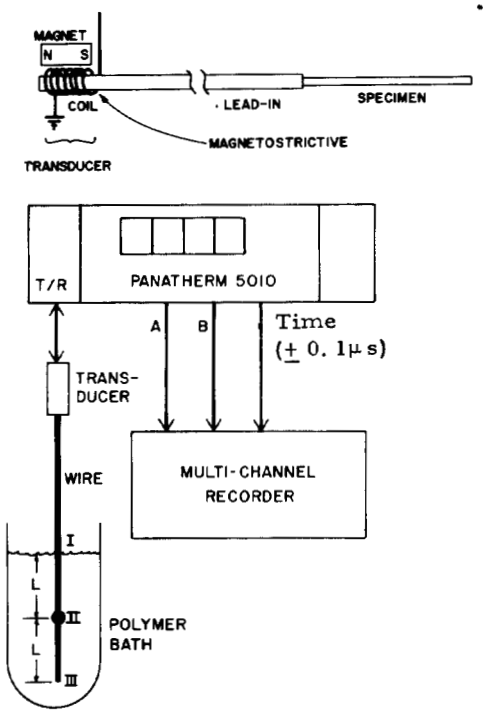

Fig. 6e. Detail of thin wire experimental arrangement to monitor polymerization automatically. The echo amplitude outputs *A* and *B* were from the weld (II) and the specimen end (III), respectively, at first. When the meniscus echo (I) grew to a preset trigger level, channel *A* began monitoring the meniscus (I) and channel *B* switched to the weld (II). After Papadakis (1974).

to vibrate longitudinally. When the vibration amplitude is attenuated to a predetermined level, another pulse is triggered. Thus the pulse repetition rate is a measure of $\eta\rho$. As ρ is usually known, η is determined. Accuracy is ~2% for Newtonian fluids. For non-Newtonian fluids, reproducibility is ~1% of full scale.

Earlier, in Poland, an ultrasonic viscometer was developed wherein a mechanical resonator was excited into the torsional mode. The decay curve was viewed on a screen, calibrated in units of η for liquids of known ρ (Filipczynski *et al.*, 1966, p. 124).

Measurements of the increasing η (along with increasing moduli) were reported about one year ago by Papadakis, for epoxy during polymerization. He utilized reflection coefficient (R) measurements of longitudinal and shear bulk waves at 5 MHz, and R and α measurements in immersed wires guiding extensional and torsional waves at ~100 kHz. The standard wire probe and readout equipment could be used for automatic measurements of η, although they were originally intended for other purposes (see Sections 2, 20). See Fig. 6e.

7. OTHER TRANSPORT PROPERTIES

Besides η, measurements of α may be interpreted in terms of the thermal conductivity coefficient K, the diffusion coefficient D_f, activation energy E, relaxation strengths S, rotational collision number Z_{rot}, etc. Direct measurements of these basic parameters are usually

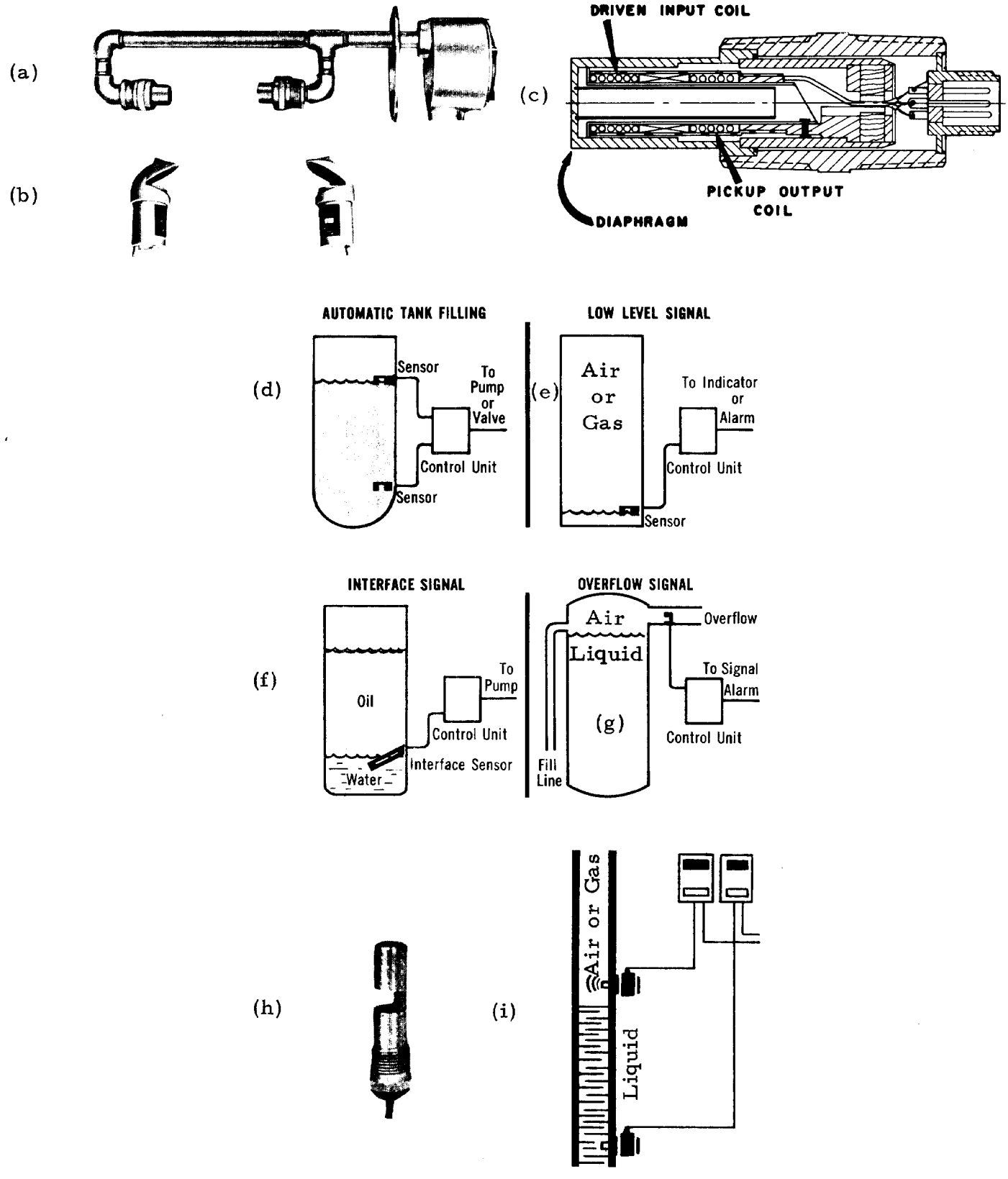

Fig. 8. Ultrasonic level measurements. (a) Transmission between National Sonics Corp. Sensall® piezoelectric transducers across 10 cm air gap is maintained until *dry* chemicals rise to interrupt beam. (b) Delavan "focalizers" operate over path lengths to ~6 m. (c) Delavan magnetostrictive single sensor resonant unit detects liquid by its dampening effect upon diaphragm. (d)–(g) Typical applications, courtesy National Sonics Corp. (h) Sensall® probe with gap. (i) Endress + Hauser "Nivosonic" probes use resonant piezoelectric element, which is dampened by liquid. Typical applications of Milltronics, Inc., noncontact AIRanger® equipment, operating at 22.5 or 41.5 kHz, include: (j) Outside storage. (k) Conveyor level. (l) Bulk storage. (m) Gyratory rock crusher. (n) Process control. (o) Liquid level. (p) Sewage level. (q) Silo load out. Use of immersed beveled probes is suggested in (r), along with a representation of an externally mounted transducer at the tank bottom, for continuous level measurements referenced to fixed reflector (*c* compensation). Side-wall externally mounted transducer senses either ring-down in wall, or reflection from inside tank, or from opposite wall (author, 1971).

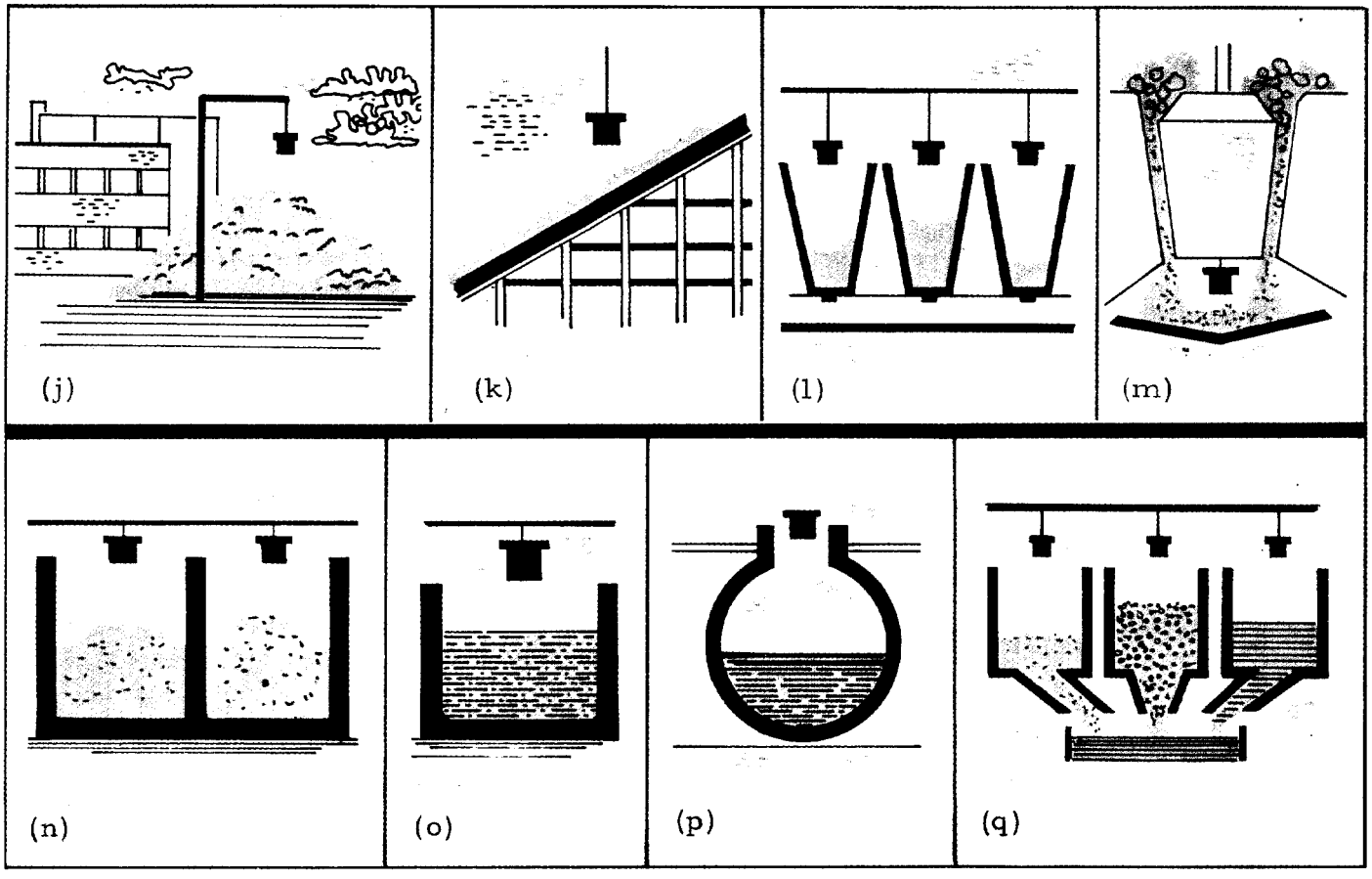

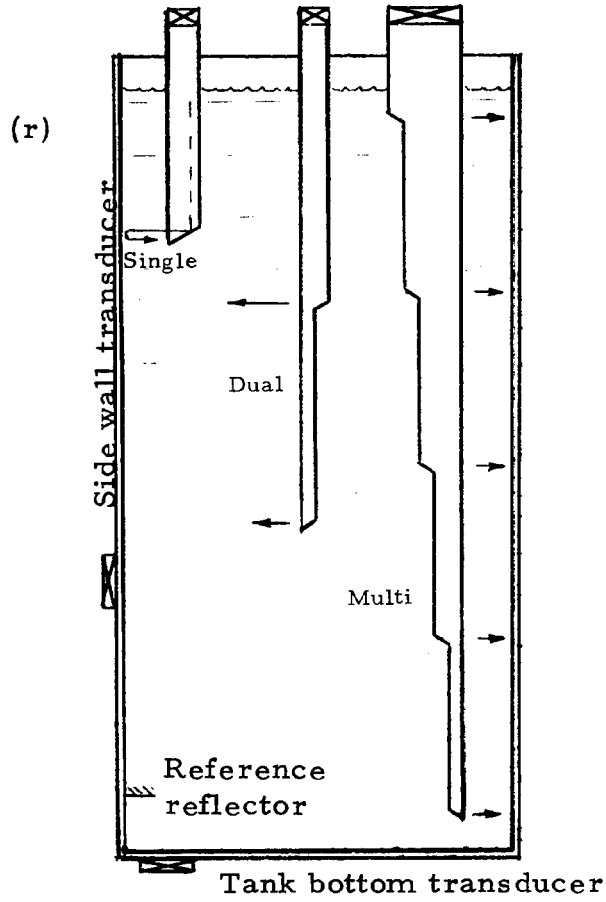

Fig. 8. *Continued.*

not considered routine industrial practice, and standard instruments dedicated to any one of these measurements apparently are not yet available. Indirect measurements of a particular transport parameter, e.g., K, are sometimes approached by empirical correlation. Such correlations can be established when c and/or α respond in a predictable manner to the same material variables that contribute to K variations in a part such as an ablative heat shield. In still other cases, mechanisms such as transport of carbon into rhenium at ~2200°C can be identified as a diffusion process, based on the time-dependence of changes in c. In one such experiment, the process, later identified as diffusion, was observed ultrasonically by monitoring c vs exposure time, when a self-heated rhenium wire was surrounded by graphite felt, in vacuum. Bell has shown that the temperature T_D above which diffuion proceeds rapidly, e.g., nitrogen into titanium, at T_D = 881°C (the "beta-transus") can also be determined by the dramatic changes in c and/or α when T_D is exceeded.

Bradshaw recently showed how η and K contributions to α can be separated, by measuring the Q of a gas-filled cavity, for different modes (radial, longitudinal). Measurements can be made for a variety of fluids, and over a wide range of T and p.

8. LEVEL

Level measurement has proven to be one of the most successful application areas for ultrasonics, with sales in excess of 1000 units annually. A recent survey in *Instrumentation Technology* (September 1974) summarized the principal ultrasonic level detectors for liquid, solid, and multiphase materials (foam, material A on B, etc.). Both invasive and noninvasive devices are widely used. Outputs can be responsive to specific levels or can indicate levels continuously.

The principal clamp-on gauges respond to presence or absence of echoes from the opposite wall, indicating the presence or absence of liquid at the transducer height. Not yet widely exploited is the damping effect of a liquid in contact with the wall. This is most sensitive for plastic-walled vessels, whose impedance is nearly matched by the liquid inside. For continuous level gauges, compensation for c changes or gradients can be achieved by a series of equidistant reflectors each positioned to reflect a small part of the incident beam (Frederick, p. 213, 1965).

Most level gauges are probe types. Resonant types are dampened when contacted by the product. Pulse types can be arranged to transmit across a gap when immersed in a fluid. Alternatively, transmission across an air gap can be interrupted by granular solids in the gap.

Noncontact types measure transit times from above the level in question. These are usually T-compensated (see Eq. (2-1)) and operate in silos, over conveyors, etc.

Experimental probes have been demonstrated by the author, wherein the transit time of an extensional wave guided by a suitable structure (e.g., a threaded plastic rod) was significantly increased in proportion to the depth of immersion in water. Also, the level of a cryogenic liquid was readily detected by the sudden reduction in the magnitude of the extensional wave reflection coefficient when the end of a dry plugged rod or Kel-F thin rod was contacted by liquid nitrogen (see Fig. 3e and Lynnworth, 1974).

Ageeva (1959) calculated and then demonstrated the change in c for flexural waves in a thin aluminum strip immersed in water. Still another approach is the use of two separately immersed probes, which may be helical wires, arranged so that the earliest arrival time of a pulse transmitted from one wire to the other is a measure of the level of the liquid which acoustically couples the pair of probes. Other concepts such as incorporating floating reflectors, floating transducers, position of a phase change in a wire, multinotched rods, etc., may be of interest in special cases. The patent literature contains many interesting approaches.

In this section it may be appropriate to include depth sounders or ocean-bottom profilers. These operate on pulse echo principles similar to the noncontact types used in silos.

Figure 8 illustrates a variety of approaches and probes for level measurement. Despite the widespread use of these ultrasonic devices, and their apparent simplicity, readers are nevertheless cautioned that application problems such as buildup, adhesion, condensation, bubbles, or other factors can sometimes frustrate an otherwise straightforward installation. Measurements in highly viscous media, or of stirred material where the top surface is sloping or curved, and measurements in the presence of moving machinery such as agitators, represent particularly difficult or impractical situations. Continuous measurements in cryogenic liquids, and in high temperature liquids such as molten sodium, have been particularly difficult, despite their apparent simplicity. Cryogenic level has been measured using thermal oscillations, i.e., the sounds of boiling when a warm solid contacts liquids such as helium or nitrogen (Laplant and Flood, 1972). Liquid sodium level was measured recently by transmission from the bottom of a stillwell (Smith and Day, 1974).

9. LOCATION OF LOW-REFLECTIVITY INTERFACES

The location of interfaces is obviously related to other categories in Table I such as level, position, and thickness, in that a distance is to be determined. In the present section, we consider interfaces between two media whose acoustic impedances are sufficiently close so that the reflection coefficient $R \ll 1$, or whose interface is so rough that coherent reflections are too weak to be detected reliably. Some petroleum products flowing in pipelines illustrate the former case, while a solidifying steel ingot illustrates the latter case. By stating the problem in terms of low reflectivity, we intend to rule out the approach of timing the reflection off the interface. The most obvious remaining approach is to use transmission, to measure c, α, or terms proportional to their reciprocals.

Transmission approaches may be nonintrusive or intrusive. Nonintrusive transducers may be mounted outside a pipe, through which liquid is flowing, or they may

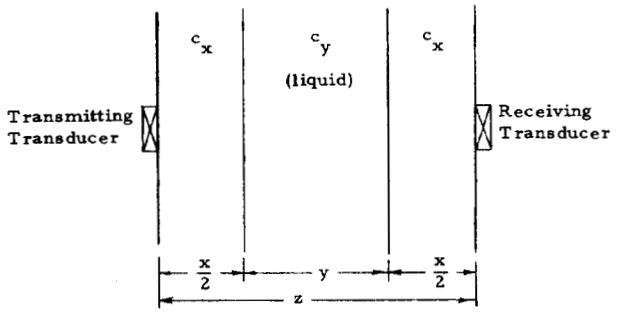

Fig. 9a. Model of two-phase layered medium through which transit time is measured.

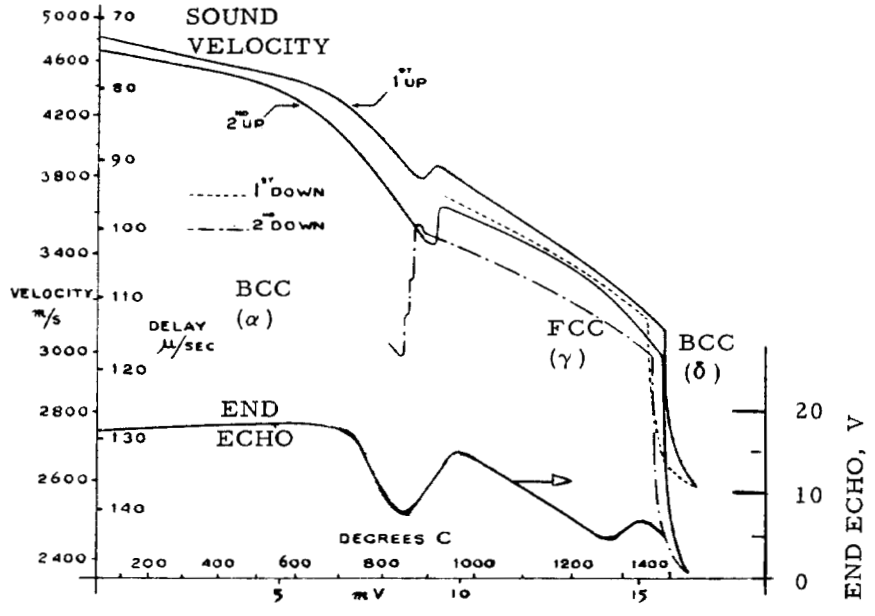

Fig. 10a. Variation of sound velocity and end echo amplitude versus temperature measured using pulse technique up to 1450°C by Hub (1962) in iron specimen of 2 mm diameter × 17 cm long, in argon atmosphere.

momentarily contact the hot exterior of a solidifying ingot. Intrusive probes such as the *c*-probe of Fig. 3c are typically mounted in a flange, penetrating the pipeline. Most commonly, the interface between two similar liquids flowing in a pipe is detected by an intrusive *c*-probe, as the interface passes the probe. For example, Zacharias (1972) has reported that in tests on 22 gasolines, there was enough difference in c so that interfaces between any two of them could be detected using a probe such as that in Fig. 3c.

A different interface location problem prevails in Fig. 9a, which is not amenable to an intrusive approach. Here we consider a layered two-phase medium. For the symmetrical sandwich or layered model depicted, suppose that sound speeds c_x and c_y as known, as is the total distance z between transducers: $z = x + y$. From a measurement of the transit time t from one transducer to another, the interface location can be determined as $x/2 = c_x(c_y t - z)/2(c_y - c_x)$. This transmission method has been used by the author *et al.* in experimental studies of steel ingot solidification, for ingots where $z \approx 20$ cm. Surprisingly, despite coarse approximations such as taking c_y as a constant for molten steel, and c_x corresponding to an average of the outside wall temperature and the solidus temperature, computations of the solid skin thickness $x/2$ based on ultrasonic data have been reasonably close to values determined independently by calipering the dumped ingot wall during solidification, and determined by computations using solidification rate theory.

The scatter observed in the transit time data corresponds to a thickness uncertainty of several mm. This uncertainty is comparable to the calculated distance between liquidus and solidus isotherms in the solidifying ingot (Jeskey *et al.*).

10. PHASE, MICROSTRUCTURE, NODULARITY

Ultrasonic measurements of c and α during phase changes in metals have been reported by Bell and his co-workers, Hub and Thorne (1962). Figure 10a is an example of Hub's 1962 work on iron, showing the influence of alpha, gamma, and delta regions on sound propagation as temperature was increased.

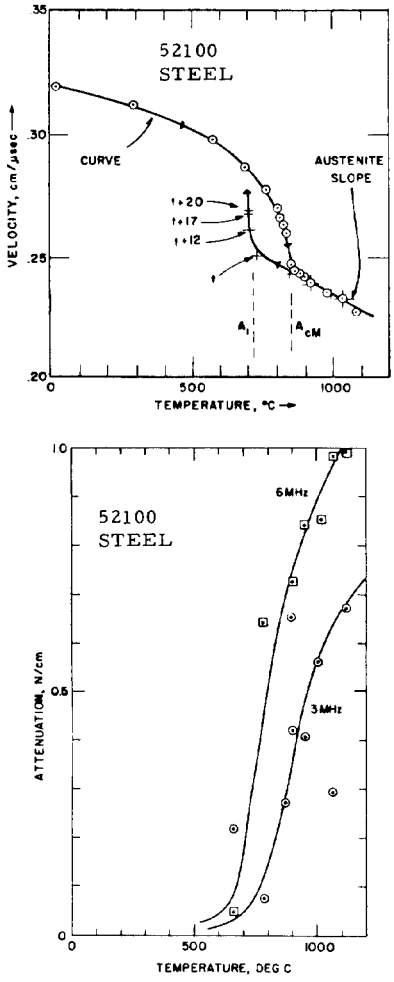

Fig. 10b. Shear wave velocity and attenuation in SAE 52100 steel versus temperature on heating and cooling. After Papadakis *et al.* (1972).

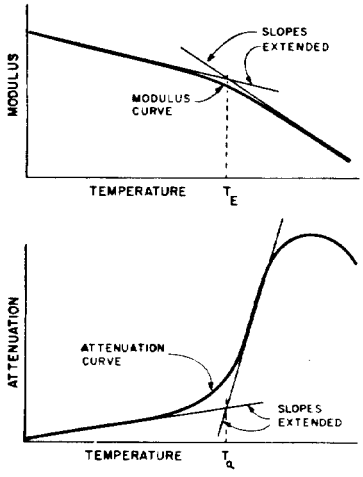

Fig. 10c. Method of defining the break points T_E and T_a in the modulus and attenuation curves. After Papadakis *et al.* (1974).

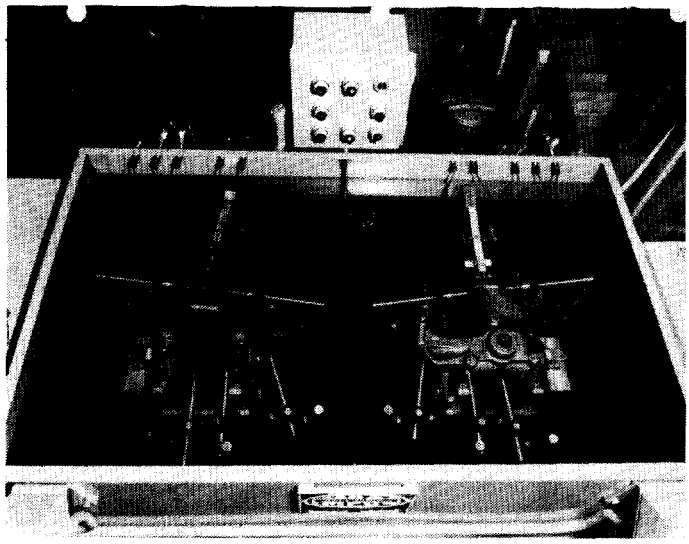

Fig. 10d. Tank, transducers, and jigging for ultrasonic immersion tests of cast iron spindle supports for the front suspension of trucks. A right-hand piece is shown, while the left-hand piece is removed to display the three transducers aimed up at critical areas to look for porosity by pulse-echo, and the two other transducers mounted horizontally for velocity measurements by through-transmission. These two transducers are aimed at a test cube for calibration; the cube pivots out of the way when the part to be tested is inserted. Ultrasonic velocity is correlated with yield strength and tensile strength in nodular iron so cast iron parts can be sorted for strength. (Illustration courtesy of Ford Motor Co.)

More recent ultrasonic studies (Papadakis *et al.*, 1972) of microstructure in steel, particularly type SAE 52100, are illustrated by Fig. 10b, where c and α are plotted vs T for shear waves. It was found that c for both longitudinal (L) and shear (S) waves dropped steeply on heating, due to the solution of carbides between the A_1 and A_{CM} temperatures. On cooling, c hysteresis is observed. This appears related to the solution and precipitation of carbides, changing the carbon concentration in the iron lattice. Below 900°C, the behavior of α_S and α_L differed, indicating different responses to possible absorption mechanisms. Above 900°C, α_S and α_L were both attributable mainly to grain scattering. This conclusion was supported by their ratio $\alpha_S/\alpha_L = 6.7$ at 900°C, in good agreement with the theoretical ratio $\alpha_S/\alpha_L = (3/4)(c_L/c_S)^3$ for Rayleigh scattering by crystallites of cubic symmetry (see also, Section 16).

In the SAE 52100 alloy work just cited, α_S remained high on cooling, indicating irreversible grain growth. But in many pure polycrystalline metals, it is found that while α increases rapidly on heating near $T_M/2$, where T_M = absolute melting point (°K), α reversibly reduces to its prior value on cooling. The observed absorption apparently correlates with a *recrystallization* mechanism, the most likely mechanism being absorption in the grain boundaries ($f < 0.2$ MHz). Further, the temperature at which the modulus vs T curve shows a break in slope, correlates with the temperature at which α vs T shows a break, Fig. 10c (Papadakis *et al.*, 1974). A potential application of such observations, would be to measure c, α, or both, as indicators of when a particular polycrystal-

line metal was above its recrystallization temperature. If one controlled T based on such a measurement, the energy necessary to hot-work a metal could be reduced in some processes. It may be of interest to note that in the laboratory, if one electrically self-heats wire specimens, the "recrystallization break points" may be identified in terms of simultaneous c and α measurements, even if T is not measured *per se*. That is to say, by increasing the heating current gradually, one can readily measure c at some (unknown or known) T near $T_M/2$, where α has suddenly increased by about an order of magnitude over its value at room temperature.

Nodularity, a specific aspect of microstructure of importance in steel castings, has been correlated with c. An example of one of several dozen installations in automobile engine manufacturing plants is indicated in Fig. 10d.

11. THICKNESS

Industrial ultrasonic measurements of thickness are most commonly made by timing the round-trip interval for a longitudinal wave pulse to traverse a sheet or plate, and converting the measured time to thickness, for materials of known c. Thousands of ultrasonic thickness gauges are now in use, operating on this principle. Digital or analog readouts are sometimes augmented by oscilloscope displays, as in corrosion studies (Fig. 11a). Rangeability is typically from ~0.2 mm to >1 m, but not necessarily in one instrument. Accuracy is better than 1%, resolution is 2.5 μm, and response time in portable instruments is typically ~1 second.

Thickness is sometimes measured by resonance techniques. For example, instruments have been available for many years to measure sheets of thickness down to <1 mm, operating on the principle that as frequency is swept, standing waves will be set up in the sheet, causing discrete indications of loading on the crystal, at a sequence of harmonic frequencies corresponding to sheet resonances. Somewhat analogously, spectral analysis of a broad-band pulse has been used to measure layer thicknesses down to ~0.1 mm (Fig. 11b).

There are also resonance thickness gauges in wide use, to monitor the film thickness of vapor deposited or sputtered coatings. Here, a quartz crystal's resonant frequency is monitored, as that crystal intercepts a sample of the coating. As the coating builds up, the frequency is reduced (Fig. 11c).

In industrial applications of pulse echo thickness gauges, special cases of unusual difficulty arise when one or more of the following conditions prevail: rough surface; curved surface; c unknown; T gradients present; thickness bounded by interface of low reflectivity for L or S waves; high α; dispersive material; material in motion at high speed; high background noise level; material surface at high temperature; thickness inaccessible (e.g., noncontactable), irregular, poorly defined, or outside the range of standard transducers or electronics.

For such special problems, less-routine supplemental approaches are sometimes considered. These include use

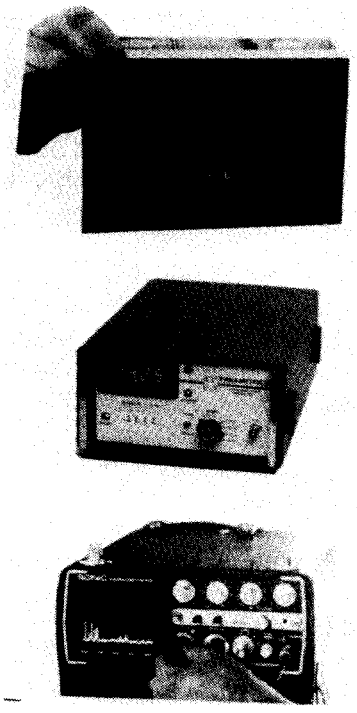

Fig. 11a. Examples of pulse-echo thickness gauges. (Top) Small size KBI "D-Meter." (Middle) Panametrics gauge measures thickness or sound speed or time interval. (Bottom) Sonic Instruments Inc. "Flaw Thickness Scope."

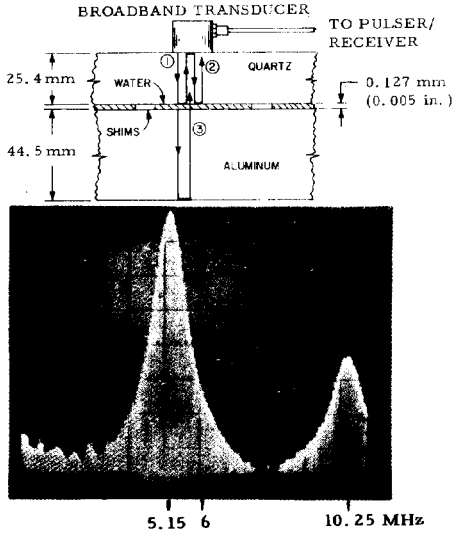

Fig. 11b. Thickness measurement of intermediate layer of relatively low characteristic impedance. (Top) Experimental arrangement. (Bottom) Spectrum of trailing end of echo 1 from fused silica/water interface, showing impulse-induced resonance. After Papadakis and Fowler (1971).

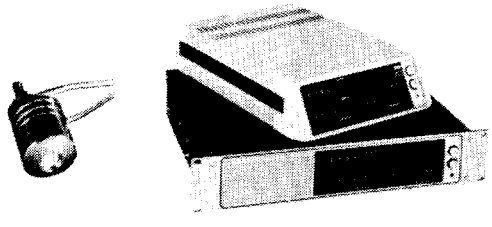

Fig. 11c. Sloan model 2000 digital deposition thickness monitors, and sensor head containing 1.27 cm diameter, AT cut, 5 MHz quartz crystal.

of: S waves, Lamb waves, Rayleigh waves, oblique incidence, focussed waves, transmission and reflection coefficients, multiple transducers, special couplants, dry coupling at high pressure, buffer rods or bubblers, frequencies well below the 2 to 10 MHz range normally employed, cw techniques instead of pulse, etc. To motivate a few of these special approaches, consider the following cases.

Measurement of Solidifying Skin Thickness: Assuming a plane interface between liquid and solid phases (an idealization seldom encountered in ingot solidification) one can compare reflection coefficients for L and S waves at normal incidence from the solid upon the liquid. For L waves, $|R_L| \approx 0.1$. For S waves $|R_S| = 1$. For this case, reflection measurements using S waves would be preferred over L waves.

Measurement When c is Uniform But Unknown, In Isotropic Material: Measurements of the critical angle by reflectivity can yield c. Then, measurements at normal incidence yield thickness.

Measurement in Presence of Unknown T Gradients: Poisson's ratio σ is a known function of T in many materials, or it can be determined experimentally, if unknown. For an isotropic material, σ can be expressed as a ratio of transit times measured for two independent modes, say, L and S modes: $\sigma = [1 - 2(t_L/t_S)^2]/[2 - 2(t_L/t_S)^2]$. From this σ, an average T is ascribed to the specimen, to which T there corresponds a specific c_L and c_S. Having determined c_L and c_S, the t_L or t_S data can be converted to thickness. Accuracy much better than 10% probably would be difficult to achieve with this method, due to propagation of errors.

Measurement of Ablation in Dispersive Composite Heat Shield: Dispersion may rule out broad-band pulse techniques. Narrow-band rf bursts or phase-coded cw may offer preferred approaches, with added potential advantages in overcoming attenuation and noise, by virtue of the narrower bandwidth.

Measurement of Sheet Material, Thickness <0.1 mm: A combination of transmission and reflection coefficient equations for very thin sheets, using the notation of Section 3, leads to an expression for thickness l of the form $l = (A/B)(Z_0/Z_1)(c/\pi f)$.

12. POSITION

In this section we briefly present three cases: position of a solid object immersed within a containment vessel; position of part of a machine such as a milling machine table or lathe carriage; position of the contact point of a writing stylus.

Figure 12a illustrates the principle of echo location of a solid object such as a stainless steel member in a nuclear reactor tank filled with liquid sodium, or a stirrer or agitator in a chemical reactor vessel. See also, Section 19, and Day and Smith (1973, 1974).

Figure 12b shows oscillograms corresponding to the position of a movable magnetostrictive wire through a

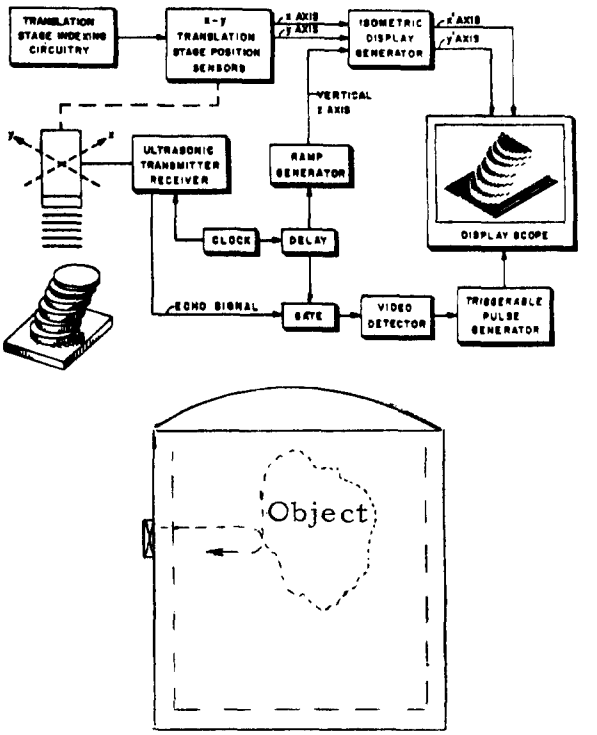

Fig. 12a. (Top) Under-sodium viewing system block diagram, after Day and Smith (1973). (Bottom) Noninvasive determination of position of submerged object.

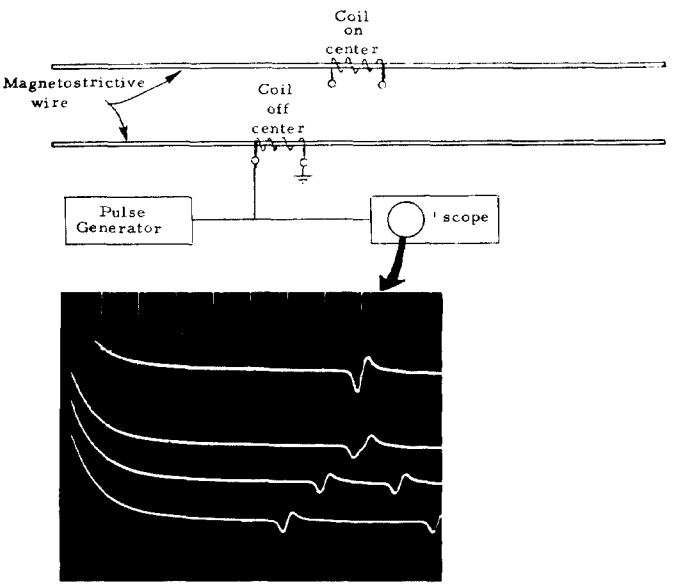

Fig. 12b. Time interval between separated pulse pair is proportional to distance that coil is off-center. Sweep approximately 10 μs/div. (Author, 1973.)

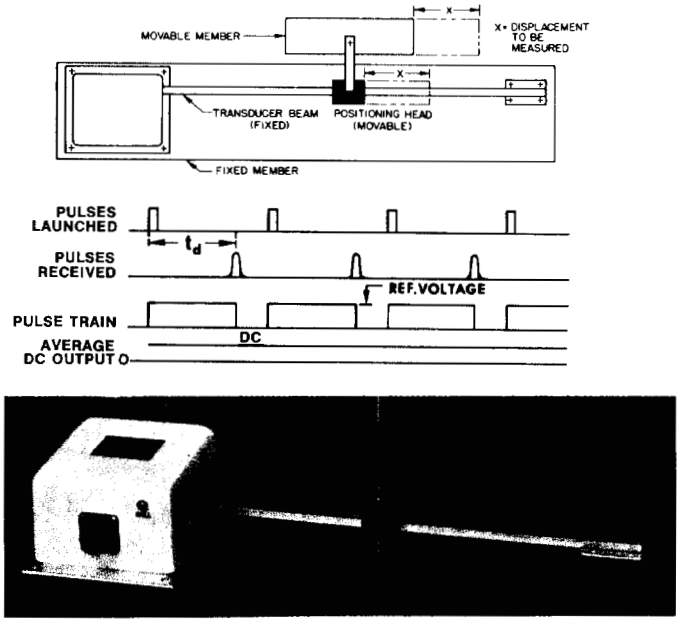

Fig. 12c. Temposonic linear displacement transducer is based on measuring time interval for an ultrasonic pulse to travel between two points on a nickel–cadmium magnetostrictive wire waveguide. The wire is enclosed in a nonmagnetic tube (transducer beam). Current pulses are applied to the wire at a quartz crystal-controlled repetition rate. By this clever version of the Wiedemann effect, ultrasonic pulses are thus generated at the position of a magnetic field intercepting the wire. These pulses arrive at a fixed reference a time interval later. (See pulse diagram.) The magnetic field is generated by a movable permanent magnet positioning head. A pulsewidth-modulated pulse train is obtained, with the pulsewidth modulated by the launching pulses and the received pulses, respectively. The pulse height is controlled by reference zeners and the pulse train is filtered to provide a DC output signal. (Illustration courtesy Tempo Instrument Inc.)

coil bobbin. If the wire is isopaustic, e.g., of the type used in T-insensitive delay lines, then the time interval between selected echoes is directly proportional to position.

Figure 12c illustrates a linear displacement device introduced by Tempo Instrument about two years ago. The device uses a nickel–cadmium wire enclosed in a measuring spar. A permanent magnet, placed on the bar at the location to be measured, magnetostrictively launches an ultrasonic pulse at the location of the magnet. The time required for the sonic pulse to travel back down the wire is measured by a quartz-crystal controlled clock and transformed into a dc output ranging from 0 to 10 volts. Ranges are available to 1.5 m, and accuracy is reported as $\pm 0.15\%$. The temperature coefficient of scale factor is less than 0.02% per °C.

Figure 12d illustrates the SAC graf/pen.® This device includes a data tablet, a stylus or cursor, and a control unit. Strip sensors on the x and y sides of the tablet receive signals from the stylus or cursor. The stylus combines a ball-point pen with a tiny spark gap. The spark generates an ultrasonic pulse. A newer model with cursor uses a piezoelectric crystal to generate inaudible ~100 kHz

® Registered trademark, Science Accessories Corp., Southport, CN 06490.

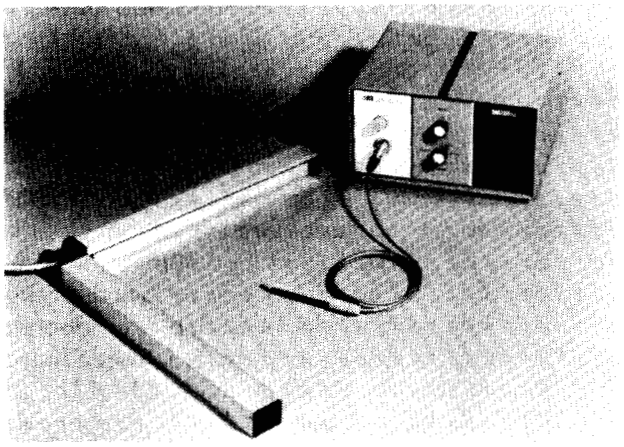

Fig. 12d. SAC "graf-pen" GP-3 digitizer. Photo courtesy of Science Accessories Corp.

pulses. The x and y travel times are digitized at rates up to 200 coordinate pairs per second and a resolution of 2000×2000 line pairs. Descriptions of numerous applications are available from SAC, some of which involve computer interfacing. Introduced in 1969, over 1000 graf/pens were sold by the end of 1974.

13. COMPOSITION

Given a mixture of two materials A and B, it appears intuitively reasonable to expect sound propagation (c and α) to bear a calculable relationship to the ratio a/b, where a and b represent the relative amounts of A and B. For simplicity we will not deal with α in this section, nor with determinations based on dispersion in c.

Given an ideal gas mixture, from (2-1) it is seen that the average molecular weight M and average specific heat ratio γ determine c at a given T. For binary mixtures, expressions for the equivalent molecular weight and equivalent ratio of specific heats are given by Noble, Abel, and Cook (1964) as well as approximations appropriate to their operation of an ultrasonic gas chromatograph for binary gas mixtures. Response is generally linear with concentration up to ~10% sample in carrier on a weight basis.

For binary mixtures of liquids, c has been measured for ~100 combinations. Empirical rules relating c to concentration or mole fraction of the added component involve Rao's constant and also Wada's constant (called the molecular compressibility). Examples are plotted in Beyer and Letcher (1969).

For "mixtures" of solids, the relationships are much more complicated. As an example, consider the modulus E of a composite containing dispersed spherical particles of modulus E_1 in a continuous phase of modulus E_0. For this case, Hashim (1962) has expressed the composite modulus as

$$E = E_0 \left\{ 1 + \frac{A(1 - E_1/E_0)F}{1 - B[E_1/E_0 + (1 - E_1/E_0)F]} \right\} \quad (13\text{-}1)$$

where F = volume fraction of the dispersed phase, and A and B are constants, with $B = A + 1$. (For other models of composites, other relationships have been derived.) Combining (13-1) with an expression for composite density ρ, the sound speed for extensional waves, for example, would be given as $c_{ext} = (E/\rho)^{1/2}$.

A standard instrument for trace gas analysis is available from Tracor, based on c measurement. He or H_2 is normally used as the carrier gas, at a pressure of ~10 to 65 psig, respectively, to provide adequate signal strength, i.e., to overcome part of the mismatch and absorption losses. Response (in degree-seconds) is a linear function of gram sample, over six orders of magnitude of the gram sample. The relative response to sample components is proportional to their molecular weights (Grice and David, 1967).

Composition measurements in many liquids are routinely conducted using NUSonics' sonic solution analyzers. Normally both c and T are measured (Zacharias, 1970). The sing-around technique is used to measure c with errors typically as small as 0.01% of reading. With careful T control or measurement, concentration can be determined in some cases to 0.02% (sulfuric acid, 85 to 100% region). Errors can increase when the liquid includes bubbles, solid particles larger than 50 μm, emulsions with large liquid droplets, and slurries. The sonic solution analyzer has also been used to determine yeast slurry *consistency* (Feil and Zacharias, 1971) and *percent solids* in foods (Zacharias and Parnell, 1972).

Composition determination in *solids* may be illustrated by an application in the glass industry (Hagy, 1973). Ultrasonic techniques for determining absolute and differential thermal expansion of titania–silica glasses have been applied to a fused sandwich seal, composed of two glasses with slight composition differences. For the titania–silica system, it was shown that for any two compositions with small titania differences the expansion coefficient differential remains constant from −195°C to 925°C. A direct correlation between ultrasonic velocity and thermal expansion was established for this glass system and led to successful nondestructive measurements. With an experimentally defined relationship, the measurement of the ultrasonic velocities yields absolute or differential expansions. Excellent agreement with seal testing data was shown to exist with differential data taken by photoelastic and ultrasonic methods.

It is interesting to note that by using a modified cell for a substitution method in the through-transmission mode, a NUSonics sound velocimeter normally used for liquid velocimetry, can be used for solid specimens too (Zacharias *et al.*, 1974).

Two *hygrometry* applications may be mentioned here. In one case, sound speed in paper and various organic materials was measured with extensional waves. As moisture levels increased, c decreased (Stungis and Merker, 1974). The second case, which represents a rather large number of proven commercial applications, utilizes a coated resonant quartz crystal as water vapor detector (Crawford *et al.*, 1964). In this sorption hygrometer, a 1 μm coating of the hygroscopic polymer is applied to the crystal. The change in resonant frequency due to the sorbed water is given by $\Delta f = \Delta f_0 \ (W/W_0)$ where Δf_0 is the frequency change due to the coating, W is the weight of water sorbed, and W_0 is the weight of the coating. To measure other vapors, different selective sorbing substances are used. A detector for UDMH, for example, is reported to respond "instantly," but requires ~1 minute for quantitative determination of concentration (Varga, 1974). Piezoelectric sorption hygrometers are available from DuPont.

14. ANISOTROPY, TEXTURE

Anisotropy influences c and α. For example, the elastic constants along different axes of single crystals have been determined from c measurements (McSkimin, 1953). Attenuation in polycrystalline solids is partly due to the discontinuities in acoustic impedance at each grain boundary.

Determination of texture, particularly in rolled materials, has been demonstrated in metals and nonmetals. Various wave types and polarizations have been used, to measure c vs direction in the specimen. Fowler (1969) showed that extensional waves could be used to determine the variation in modulus in rolled Ti sheet, in specimen strips cut with axes at 0°, 45°, and 90° to the rolling direction. Martin (1968) suggested that a quartz shear wave crystal and a Q-meter could be used to show that, as the crystal was rotated, the resonant frequency extrema for rolled sheet metal would correspond to polarizations parallel and perpendicular to the rolling direction. Papadakis (1973) demonstrated line-contact coupling for determining texture in paper, and later (1974) demonstrated ultrasonic spectroscopy as applied to the calculation of the texture parameter $\Delta c/c$ for rolled aluminum.

15. NONDESTRUCTIVE TESTING

This section identifies a few examples in the category variously labeled NDT, NDI (nondestructive inspection), or materials evaluation. Topics commonly included under these labels are the determination of flaw size, shape, and distribution; inclusions; voids; cracks; delaminations; disbonds; and other departures from specifications. Other items in Table I, such as items 10–14, and 16–20, also could have been grouped in the present section.

Topics included in NDT represent the activity of thousands of workers over the past 35 years. A number of books, journals, and professional societies are devoted exclusively to these topics. Annual sales of NDT ultrasonic equipment are well in excess of $10M. Therefore it is clear that any attempt to summarize briefly the scope of NDT technology and equipment would be inadequate.

For those readers unfamiliar with NDT practice, it may be of interest to note that ultrasonic tests are most often confined to the 1 to 10 MHz decade. Longitudinal wave pulses are principally used. The transducer is usually

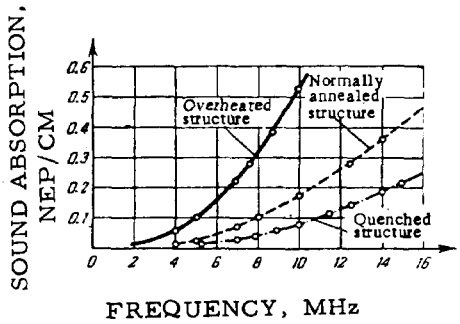

Fig. 16a. Dependence of the absorption of ultrasound on frequency for steel subjected to various heat-treatments, after Babikov (1960).

housed in a case, such that pulses can be coupled manually either through a thin film of liquid (contact test) or through a substantial distance of water (immersion test) such that the test piece is in the far field. The same transducer serves as transmitter and receiver in most cases. Focussed waves at frequencies as high as 50 MHz are used in some high-resolution tests. Angle beam and buffer rod techniques are also used. Electronic equipment usually consists of a basic pulser/receiver and oscilloscope, plus various additional or optional items such as gates, alarms, analog or digital displays, recorders for scans, etc. Additional details are contained in the bibliography.

16. GRAIN SIZE IN METALS

The dependence of the attenuation of ultrasound on the grain size of metals and alloys has been studied over a wide range of frequencies. The different structures and correspondingly different grains in test samples are often obtained by using different heat treatments. The experimental data confirm the theoretical conclusions relative to the increase in attenuation with increasing frequency and grain size.

As Babikov (1967) notes, in polycrystalline bodies the sound-scattering mechanism at relatively low ultrasonic frequencies (of the order of a few MHz) is similar to the scattering of sound by fine-grained particles, and at high frequencies it becomes similar to the process of diffusion. In the determination of grain size in metals by the ultrasonic method, one should utilize those frequencies at which the absorption of ultrasound is strongly dependent on the grain size.

For the practical application of the ultrasonic pulse method of measuring the grain size in metals and alloys, Babikov recommends the following frequency range: the upper limit of the applied frequencies is suitably bounded by a wavelength equal to or somewhat greater (by a factor of two or three) than the grain diameter, while at the lower limit, the wavelength should exceed the grain diameter by a factor of 15–20.

The study of ultrasonic absorption in steels is of considerable practical interest. For construction and instrument steels, heat treatment proves to have the greatest influence on the ultrasonic attenuation. It follows from Fig. 16a that quenched steel has the lowest absorption. On the other hand, for an overheated structure, which has the distinguishing feature of a large grain size, the absorption of sound is much greater. Thus the ultrasonic method could be utilized in quality control of the heat treating of a metal.

17. STRESS AND STRAIN

A number of ultrasonic studies have been aimed at evaluating residual stress in metals, based on changes in c with stress. Unfortunately, factors other than stress (e.g., inhomogeneities, texture) influence c too, and unless the effects of these other variables can be eliminated or compensated for, the satisfactory determination of internal stresses remains elusive.

If a specimen can be interrogated over a given path before and after the stress is applied, the value of the stress can be resolved to better than $\sim$100 psi. The limit on resolution depends on material, wave type (L or S), propagation direction, and polarization relative to the stress axis, and on the resolution limit of the electronics. Sing-around and pulse-echo-overlap methods have been used to resolve c changes of 10 to 20 ppm.

It is interesting to compare ultrasonic sensitivity to stress with strain. Hsu (1974) presents data for 1018 steel and 2024-T4 aluminum. For the steel, using 10 MHz shear waves propagated perpendicular to the compressive load direction, but with particle motion parallel to load direction, Hsu measured c increases of 0.1% per 20 000 psi. The strain equals the stress divided by Young's modulus, or about 0.07% for the 20 000 psi (1.38×10^8 N/m^2) stress. Thus the change in c due to stress is about 1.5 times the strain.

Can one apply the above type of data to measure the tension in a bolt, with access to the head? Not easily. If the bolt is faced off square to the axis at both ends, and is available for measurement before and during tightening, and there are no significant T changes, the task becomes more reasonable. Note that now the propagation direction is parallel to the load direction. Also, the transit time changes due to stress and also due to strain. Krautkramer (1964) discusses this application, with reference to a carbon–steel bolt where the effects of stress and strain are additive. In practice, use of an oscilloscope with delayed expanded sweep enabled the operator to control bolt tension by tightening until a predetermined fractional increase in round-trip transit time was observed.

A rather specialized means for recognizing *torsional* stress in magnetostrictive wires or rods was discovered accidentally in remendur which had been straightened by a rotating-jaw machine (Lynnworth, 1972). It was unexpectedly observed that in wire thus straightened, torsional wave magnetostrictive transduction was strong, and relatively uniform and permanent, compared to the Wiedemann effect normally induced by electrically magnetizing a wire circumferentially. Heating the straightened wire red-hot for a few seconds relieved the torsional stress,

as indicated by the observation that such heat treatment eliminated the torsional transduction effect in the heated segment of the wire.

18. ACOUSTIC EMISSION

A few years ago, the president of the Acoustical Society of America predicted that acoustic emission would be the fastest growing field in acoustics during the seventies. Halfway through this decade, one can see international activity in acoustic emission. Symposia, books, over 300 journal articles, special issues, newsletters, an acoustic emission working group, an ASTM subcommittee E07.04, several organizations entering the field, existing companies enlarging their facilities, introduction of equipment of increasing sophistication, calibration standards—all these indicate increasing interest and industrial acceptance of acoustic emission as a means of monitoring potential failure mechanisms in critical parts or structures.

Acoustic emission (AE) systems "listen" to materials and structural phenomena by amplifying, filtering, recording, displaying, and analyzing signals emitted by the phenomena. Welds have received considerable AE attention, both after and even during the welding process. Well-known applications are found in the nuclear, petrochemical, and aircraft industries, and also in monitoring bridges, buildings, and even wooden beams.

Well-documented AE studies include other areas such as: martensitic phase transformations, dislocation processes, fiberglass and whisker reinforced composites, fracture mechanics, plastic deformation, crack growth during hydrogen embrittlement, stress corrosion cracking and low cycle fatigue, and detection of unwanted particles inside sealed transistors. Sonic signature analysis has been used in monitoring bearings. See Liptai *et al.* (1972) in Ref. [18a].

Instruments are available to locate cracks by triangulation, to measure count rates, to discriminate against noise, and to analyze the amplitude distribution of signals.

Calibration devices and test sets to verify triangulation programs have utilized phase changes, extensional waves coupled via a sewing needle point, and sparking.

Details on specific applications are given in the bibliography and in literature available from AE system vendors. (See also, Sections 21, 22.)

AE "dosimeters," or ultrasound level meters, may be required as safety equipment in areas falling within the provinces of government or consumer regulatory agencies such as BRH, FCC, FDA, OSHA, or CPSC.

19. IMAGING, HOLOGRAPHY

Fundamentally, it is not essential to convert information about a test specimen from acoustical waves to light waves, in order to make decisions concerning the location, size, shape, orientation, or motion of detected inclusions. Bats have proven this. However, for most operators of ultrasonic test equipment, a visual image is desirable. The various oscilloscope or scan-recording modes, including those which give an appearance of perspective, provide some degree of imaging, in effect. Sokolov's (1934, 1950) image converter is described in various texts (Blitz, 1967, p. 199). Displays now can be on an oscilloscope or TV screen. The possibility of using color on a TV display to represent acoustical information has been suggested. For example, spectral, intensity, or phase information could be represented. Schlieren methods have been used to visualize sound waves. Powder methods are familiar to many students of acoustics, to demonstrate standing wave patterns. Acoustical/optical interactions in certain crystals have been described.

At the moment, the most important industrial coherent method for visualizing ultrasonic targets appears to be acoustical holography. In holography, both amplitude and phase information of the wavefronts emerging from the flaw are usually recorded in terms of light intensity on film. The hologram or coded interference pattern contains the diffraction information necessary to reconstruct the original flaw wavefronts and thus produce a true visible image of the flaw.

Within the past decade, a number of reports have appeared on the use of holography for inspecting thick-walled pressure vessels, locating and identifying submerged objects and for other NDT applications (Collins, 1973). Biomedical applications, although beyond the scope of this review, are important, and well-documented. Several organizations have built holographic or other imaging systems, which may in time become standard products. Holosonics introduced their holographic equipment in 1971, and about 30 NDT systems have been sold to date.

Sokolov imaging equipment was manufactured by James Electronics several years ago, but after some seven systems were sold, it was decided to withdraw this product from the commercial market.

One can categorize imaging equipment performance in terms of the resolution being on a macro scale or micro scale. If we define microresolution to mean resolution on the order of 0.1 mm or less, then most imaging and holographic equipment can be said to resolve in the macro scale. Holosonics' system 200, for example, provides a 3D focussed image in real time, essentially achieving the theoretical half-wave resolution limit. For common metals, tested below 5 MHz (S waves) or 10 MHz (L waves), $\lambda/2$ exceeds 0.1 mm.

RCA has been developing a system whose resolution is now approaching the micro border, namely ultrasonovision (Mezrich *et al.*, Vilkomerson, 1974). Ultrasonovision is a large aperture high resolution system for the visualization and quantitative analysis of acoustic wavefronts. It is based on a Michelson interferometer in which one mirror is a thin metallized pellicle submerged in water and through which passes the acoustic wave (see Fig. 19a). A scanned laser beam is used to rapidly measure and display—presently with a sensitivity of 0.05Å—the displacement amplitude of the acoustic wave. Stability of the interferometer is obtained by modulating the length of the reference leg. An optical arrangement allows acoustic apertures of 150 mm using a minimum of large optical

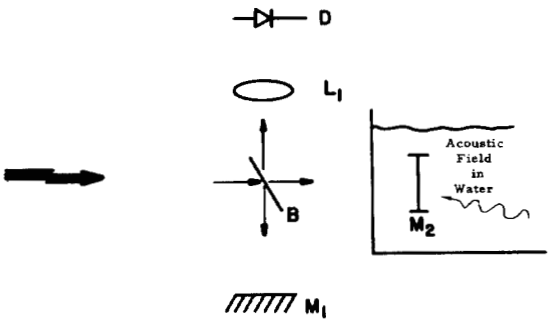

Fig. 19a. Basic arrangement of Ultrasonovision system. B is a beam splitter. M_1 is the rigid external mirror, M_2 is the flexible mirror or pellicle. L_1 collects the light from the interferometer onto the photodiode D. After Vilkomerson (1974); courtesy RCA.

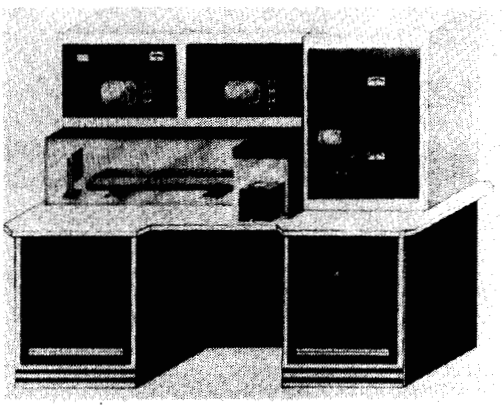

Fig. 19b. The Sonomicroscope is a 100 MHz acoustic microscopy apparatus with built in TV monitors for real time simultaneous acoustic and optical visualization of a specimen. Videotape equipment may be built into the desk. The specimen is placed on the stage, where it is insonified. The stage is positioned under the scanning laser beam probe which is located to the left of and slightly behind the stage. Courtesy Sonoscope Inc.

components, and permits system resolution below a millimeter. The system has an acoustic angular response flat over a 50° half angle and a uniform frequency response to at least 10 MHz.

On the micro scale, Zenith Radio Corporation developed a concept for an acoustic microscope (Korpel, Kessler, Palermo, 1971, 1972, 1973). By producing images of *microstructural* detail, it opens up a new dimension in ultrasonic visualization. The instrument, which is being manufactured and marketed through Sonoscope Inc., is known as the Sonomicroscope and is shown in Fig. 19b. In order to achieve resolution in the micron size range, high acoustic frequencies, typically 100 MHz and above, are employed. Furthermore, high resolution detection is accomplished by a noncontacting focused laser beam probe which is rapidly scanned to produce real time acoustic micrographs.

Applied to both the material and biological sciences, the Sonomicroscope reveals information on structure which directly pertains to variations in density and elasticity on a microscopic scale. Grain boundaries may be observed in the bulk of a material for example, as well as microfractures, inclusions and disbonds. Furthermore, by

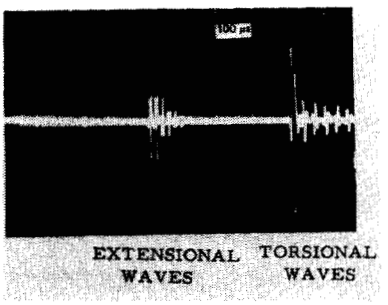

Fig. 20a. Simultaneous magnetostrictive generation of extensional and torsional waves is used to measure elastic moduli and Poisson's ratio in slender rod or wire specimens. After Lynnworth (1972).

employing the interference mode of operation localized stresses may be revealed.

For further details the reader may consult the growing body of holography literature.

20. ELASTIC PROPERTIES

Equations relating sound speeds for appropriate modes and polarizations to corresponding elastic constants, elastic moduli, and Poisson's ratio are available in numerous texts, and so are not repeated here. For industrial applications, ultrasonics provides a well-established way of obtaining the required data, for temperature from cryogenic levels up to the melting point or destruction temperature of the specimen. Measurements of c in loaded specimens provide data on higher order elastic constants (see also Section 17).

Measurement techniques include resonance and pulse. Magnaflux has marketed the "Elastomat" resonance equipment for many years. Cylindrical test specimens, typically $\lesssim$1 cm diameter $\times$ $\sim$10 cm long are supported at nodal positions. The resonant frequency typically is measured as a function of T, up to $\sim$1000°C. With appropriate furnace, coupling members, and refractory specimen, resonance techniques have been used to over 2500°C. Resonant frequency of carbon sheet steels is indicated by Control Products Company's Modul-$\bar{\Gamma}$ drawability tester.

A wide variety of pulser/receiver combinations have been devised for elastic property studies, and also a variety of specimen configurations, especially for high temperature studies. The principal configurations or experimental approaches for high temperature moduli studies in solids using pulse techniques are the notched bar (Frederick, 1947); the notched wire (Bell, 1957); use of mode conversion to obtain shear wave data (Reynolds, 1953); and momentary contact (Carnevale *et al.*, 1964). Frederick's method has been used at Sandia in recent studies of graphite to $\sim$3400°C. The author combined Bell's method with electrical self-heating to obtain moduli data in Mo, Re, and W at the melting points of these metals, 2610, 3180, and 3410°C, respectively (Lynnworth, 1968). Bell's method underlies the design of the Panatherm 5010, a pulser/receiver/time intervalometer instrument which is used in about a dozen different laboratories for moduli

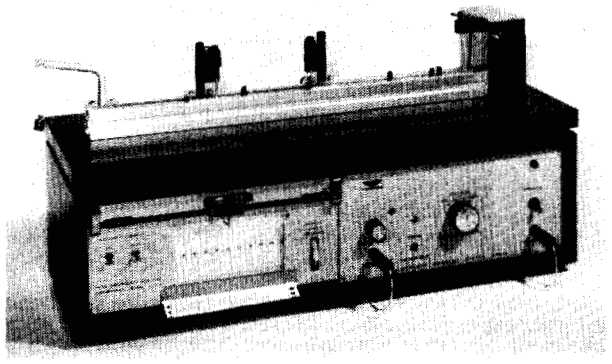

Fig. 20b. Dynamic Modulus Tester PPM-5R shown with Fiber Scanner Option. The Fiber Scanner Option is used for testing natural and synthetic fibers such as polyester, nylon, cotton, spandex, hair, etc. Photo courtesy H. M. Morgan Co.

determinations (Lynnworth, 1973). Echoes from which Young's and shear moduli can be obtained simultaneously are illustrated in Fig. 20a.

In general, routine ultrasonic methods are applicable to a large number of materials and geometries. However, specimens which are dispersive by virtue of their inhomogeneous construction or bounded geometry are not easily evaluated by routine procedures. To measure dispersion, i.e., variation in phase velocity vs frequency, variable path and/or variable frequency techniques may be required. Illustrations of phase and group velocity measurements, and of the potential interpretive errors attending the uncompensated use of pulse techniques in dispersive specimens, are contained in Thompson (1973) and in Lynnworth, Papadakis, and Rea (1973). The former work relates to Lamb waves in steel plate; the latter to L and S waves in woven reinforced composites.

For laboratory and also for on-line measurements of elastic modulus in fibers, filaments, films, and papers, H. M. Morgan Company's dynamic modulus tester (Fig. 20b) has been widely used for over ten years. A bibliography relating to this tester, containing over twenty references, is available from H. M. Morgan. About 300 of these instruments are in use.

Transit time measurements obtained with the James Electronics' "V"-Meter monitor the setting of concrete; respond to c and thereby match graphite electrode sets to control their burning rate; etc. Transmitted frequencies are ~50 to 150 kHz for small specimens in the lab, and ~25 to 50 kHz for large structures encountered in the field.

21. BUBBLES AND PARTICLES

Detection and measurement of bubbles and particles is important in industrial areas such as heat transfer, fuel lines, liquid transfer, instrumentation lines, etc. Discontinuities of these types influence c and α, and in principle can be detected by pulse-echo, transmission, or scattering (e.g., Doppler) methods, and sometimes by passive methods.

In 1971 Vero Precision Engineering Ltd. introduced a bubble and particle detector comprised of a transmission cell and an electronic module. However, the instrument is no longer manufactured, at least not in its original form. Albertson and Van Valkenberg's 1964 paper on ultrasonic detection, sizing and counting of subsieve particles is summarized in Frederick's book, pp. 239–241 (1965).

Detection of water boiling is readily demonstrated with simple pulse-echo equipment (Lynnworth, 1971). However, under realistic conditions, where in fact *incipient* boiling is to be detected, the problem is much more difficult. Acoustic detection of boiling in liquid sodium at temperatures up to 650°C, has been approached by using lithium niobate transducers operated as acoustic emission (AE) receivers (see also Section 18), as reported by Anderson *et al.*, (1972).

Response to particles underlies Doppler blood flowmeters, the particles being the red corpuscles. Accordingly, one investigator used a standard Doppler flowmeter to measure the flow velocity of scatterers in liquid metals (Fowlis, 1973). Possibly, similar equipment will be found effective in detecting or measuring scatterers such as bubbles, particles, or other contaminants.

22. GAS LEAKS

As pressurized gas escapes through an aperture it creates considerable ultrasonic noise, in particular, within the band 36 to 44 kHz. The Delcon Ultrasonic Translator Detector (such as Model 4905A) manufactured by Hewlett-Packard's Delcon Division, detects this characteristic sound with a directional barium titanate microphone and translates the signal to audio by mixing it with a 40 kHz local oscillator signal. The audio signal is then amplified and monitored on a speaker and level meter. See Fig. 22a.

To detect leaks in aerial cables, the equipment operator merely scans the cable from the ground with the flashlight-size microphone, listening for the characteristic hissing sounds of a leak. By simultaneously observing the level meter, one can "peak in" on the leak and determine its exact location. Pole mounted accessories are also available for closer scanning of the cable.

Leaks in ducted underground systems are located with a "Duct Probe" accessory. Consisting of a miniature microphone connected to a system of aluminum rods, the Duct Probe can be used to explore up to ~150 m (500 feet) into a cable conduit. The leak is thereby pinpointed, permitting repair of the damage with a minimum of excavation.

About two years ago Dukane introduced their model 42A15 ultrasonic leak detector, designed primarily for checking telephone cable leaks.

Capable of locating air, gas, and corona discharge leaks the self-contained 24 oz (0.7 kg) unit (Fig. 22b) detects ultrasound in the frequency range 38–42 kHz. Sensitivity is 6 dB signal-to-noise ratio at 6–8 ft (1.8–2.4 m) from a leak source consisting of a 0.005 in. (0.13 mm) orifice subject to a 2 lb. in.$^{-2}$ (13.8 kNm^{-2}) pressure head.

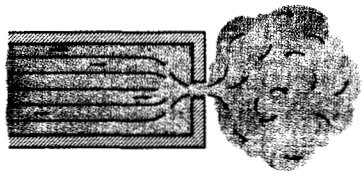

Principle of noise generation

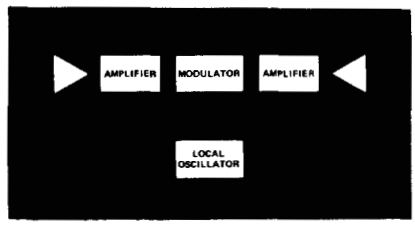

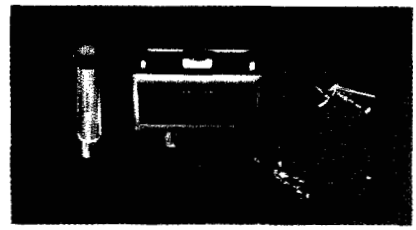

Fig. 22a. (Top) Ultrasonic noise is produced by turbulence of leaking gas. (Middle) Block diagram underlying "frequency translation" into audible range. (Bottom) Model 4917A. Illustration courtesy Delcon Div./Hewlett-Packard Co.

Fig. 22b. Leak detector with headset, model 42A15, by Dukane Corp.

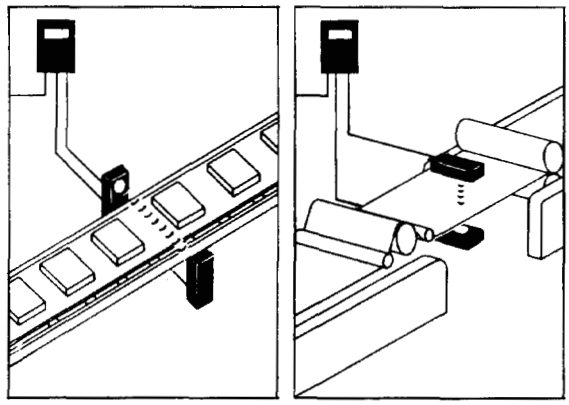

Fig. 23a. Applications of interrupted sound beam, courtesy Endress and Hauser.

The power source is a 9 V transistor battery giving 40–50 hours normal operation, but an equivalent mercury battery is available giving up to 100 hours service. Output is monitored through a high noise level headset using a thumb operated sensitivity control. The complete unit is contained in a rugged splash-proof housing and can be fitted with the Bell system parabolic reflector for long-range overhead detection.

For gas leaks under liquid, the bubble-detection methods of the previous section may be considered.

23. COUNTING WITH INTERRUPTED SOUND BEAM

Moving objects can be counted as they interrupt a beam of ultrasound. In one system, an ultrasonic beam with a frequency of approximately 40 kHz passes between transmitter and receiver. The beam is interrupted as an object comes between transmitter and receiver, producing a signal which is used to de-energize a relay in a remote power supply. The transmitter and receiver each employ piezoelectric crystals. As an ultrasonic beam hits the receiver membrane the built-in piezoelectric crystal converts the mechanical vibration into an electric oscillation. This oscillation is fed back into the circuitry. As the vibration ceases, the circuitry is detuned to de-energize the relay in the power supply. The receiver has a built-in adjustment potentiometer to adjust the system to different distances. The maximum distance between transmitter and receiver is ~3 m (10 feet). The ultrasonic beam diameter can be reduced by means of cones and similar focussing devices to achieve higher sensing resolution. These devices make it possible to detect objects as small as 1.5 mm, up to an object the size of a railroad freight car.

Typical applications are illustrated in Fig. 23a. Proven applications include: counting or signaling on production lines, conveyor belt monitoring, breakage warning in paper mills, and edge or width control. See also: Frederick, p. 215 (1965).

24. BURGLAR DETECTION

Intruders entering a defined region are recognized by their interrupting or reflecting a beam (see Section 23) or by their disturbing a field of ultrasound that is established in a volume such as a room. It appears that transmission, reflection, scattering, and frequency-shift approaches are appropriate for this type application.

25. OTHER APPLICATIONS

Some industrial applications other than those covered in the previous Sections 1–24 are mentioned in Frederick's book (1965), such as quality of milk, hardness of metals, signaling, acoustic logs, delay lines, guidance devices for the blind, odometer/speedometer, and displacement of a vibrating surface.

From Adams' 1974 book *Conceptual Blockbusting*, it is understood that one easy way to "create" new devices

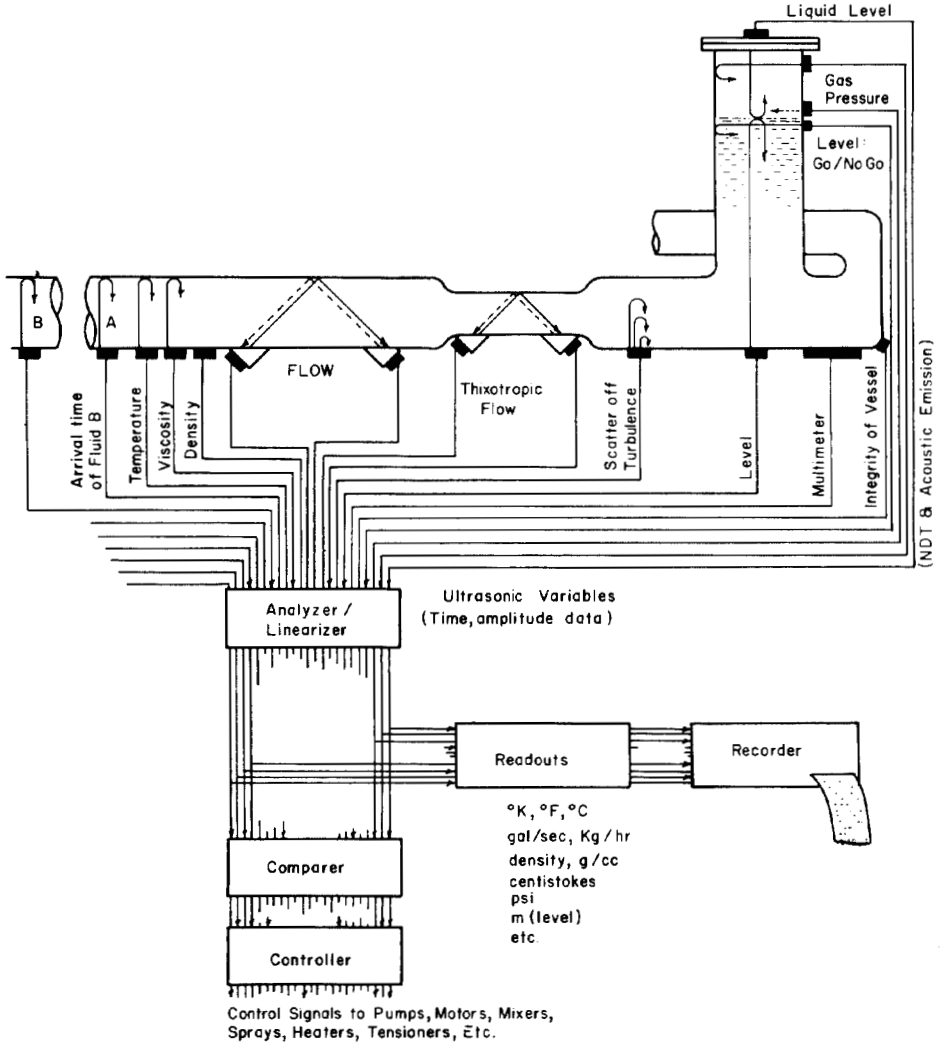

Fig. 25a. Schematic of ultrasonic instrumentation system for fluid process measurement and control.

is to combine existing devices. (The technical or commercial success of such combinations, unfortunately, cannot be guaranteed.) Examples of potentially or actually useful combinations include measurements of: mass flow rate $\dot{M}$, as the product of density ρ and flow velocity v; volumetric flow rate, in unfilled channels or conduits, by combining v, liquid level, and a channel shape parameter; kinematic viscosity $\nu = \eta/\rho$, where η = viscosity coefficient; flow and temperature, from sums and differences of simultaneous upstream/downstream transit times in flowing media, etc. Combinations of ultrasonic level measurements with nonultrasonic data such as geometry of a tank, can yield tank ullage, that is, the vacant volume, above the liquid, which is important in cryogenic fuel handling. A combination of ultrasonically-determined v with gamma-ray-determined ρ has been used to measure $\dot{M}$ for airborne coal dust. Energy content meters for cryogenic fuel are now under evaluation, which may include combinations such as a vortex shedder for v, a resonant vane for ρ, and a calorimeter for energy content per unit mass.

Clearly, the number of combinations is astronomical. As advances are recognized in different fields, such as LSI circuits, low-cost computer chips, high temperature piezoelectric materials, medical ultrasonics, etc., new and useful combinations may be expected to mature and grow from the conceptional level to the industrial world, that is, from the theoretical to the applied domain.

CONCLUSIONS

It appears that the quartz crystal is still playing a starring role in ultrasonics, nearly a century after its first role in the story of piezoelectricity. Despite numerous man-made ceramics having higher activity, sensitivity, dielectric constant, operating temperature, etc., quartz is still the choice for the sensing element in cases where the loading can be determined by the reduction in resonant frequency. In these nostalgic times one can predict that still more roles will be identified for this seasoned performer.

On the other hand, numerous applications await the reliable and/or novel coupling of other transducer mate-

rials to problems of commercial interest. These applications require not only the efficient transmission of sound between the transducer and the material under investigation, but also an understanding of the interaction of ultrasound with the parameter of interest. Interactions with the undesirable variables or constraints normally present in industrial situations, must also be understood.

Intrusive probes are used more often than nonintrusive externally mounted, nonwetted transducers, in most types of applications. The main reason for this is that insertable probes are more easily designed to be responsive primarily to the parameter of interest, yet be relatively immune to other variables. Also, the skills required to install or use a rugged probe, are readily available in many user facilities, whereas the proper installation of externally mounted transducers sometimes requires experience and skill in the art of ultrasonic coupling. In any event, the user should understand the conditions required for satisfactory operation. When these conditions are not met, disappointing performance is to be expected.

In principle, most of the industrial applications preivously mentioned can be approached with a suitable combination of transducer(s), pulser or oscillator, receiver, a time intervalometer, phasemeter or voltmeter (e.g., peak detector), and a calculator to convert the raw c, α, or related data to the user's customary units of measure. In practice, such a general approach is confined to laboratory, experimental, or feasibility studies. Practical solutions consist of optimized combinations tailored to a specific parameter, in most cases.

Standard equipment is available for many specialized applications, as well as for the principal variables in process control, namely, flow, temperature, pressure, level, density, and viscosity. Large companies are already involved in marketing equipment for determining these parameters ultrasonically. More companies may be expected to follow, especially in the area of flow, and possibly temperature, where markets are defined and known to be large enough to warrant the risks attending the introduction of new products.

Technological forecasting partly involves recognizing needs in industry, and correlating these needs with potential solutions from research laboratories and/or from manufacturers willing to invest in, develop, market, and service new products. The energy, material quality, ecology, and economic situations in the next few years are likely to provide strong motivating factors, defining the need for new or better products, techniques, or services. This includes a need for measurements to higher accuracy, with statistically defined error bounds, and measurements with less labor involved in the installation and maintenance of equipment, and with less subjective, more automatic, and rapid interpretation of data. The potential of noninvasive externally mounted ultrasonic multiplexed transducers, linked to a minicomputer as in Fig. 25 suggests one avenue along which progress may be responsive to the above needs anticipated in industry. Traffic along this avenue is already discernible.

ACKNOWLEDGMENT

The author gratefully acknowledges numerous helpful discussions with and suggestions from his colleagues, as well as with manufacturers of the ultrasonic equipment discussed above. Manufacturers have kindly provided illustrations and also other unpublished sales data which help identify the degree of acceptance of certain applications in industry.

BIBLIOGRAPHY

(By the Section Numbers)

[1a] A. del Grosso, NRL 4967 (Nov. 1957); AD149409.
[1b] R. B. Dowdell, ed., *Flow—Its Measurement and Control in Science and Industry*, Vol. 1, ISA (1974), particularly pp. 897–960.
[1c] L. C. Lynnworth et al., in: *Proc. IEEE Ultrasonics Symposia* (1972, 1973, 1974).
[1d] N. Suzuki, H. Nakabori, and M. Yamamoto, pp. 115–138, in: C. G. Clayton, ed., *Modern Developments in Flow Measurement*, Peregrinus (1972).
[1e] *Ibid*, S. G. Fisher and P. G. Spink, pp. 139–159.
[1f] B. G. Liptak and R. K. Kaminski, *Instrum. Techn.* 21 (9), 49–50 (Sept. 1974).
[1g] M. Luukkala and P. Meriläinen, *Ultrasonics* 11 (5), 218–221 (Sept. 1973).
[1h] H. Frankenberger, B. Grohs and E. Häusler, pp. 682–683 in: *Proc. IEEE Ultrasonics Symp.*, IEEE Cat. #74 CHO 896-1SU (1974).
[1i] L. C. Lynnworth, *Materials Eval.* 25 (12), 265–277 (Dec. 1967); U. S. Patent No. 3,477,278 (Nov. 11, 1969).
[1j] EDO Corp., *Chem. Engineering*, p. 54 (Nov. 25, 1974).
[1k] N. E. Pedersen *et al.*, NASA CR-112313 (June 1973); USAAMRDL—TR-75-8(1975).
[2a] H. H. Plumb, ed., *Temperature—Its Measurement and Control in Science and Industry*, ISA (1972), particularly Part 1, pp. 689–732.
[2b] J. G. McMillan and R. H. Pamperin, SAE Paper 720158 (Jan. 1972).
[2c] J. F. W. Bell, *Phil. Mag.* (8) 2, 1113–1120 (1957).
[2d] J. R. Frederick, Ph.D. Thesis, U. of Michigan (1947).
[2e] K. A. Fowler, US Patent No. 3,595,069 (July 27, 1971).
[2f] S. S. Fam, US Patent No. 3,540,279 (Nov. 17, 1970).
[2g] L. C. Lynnworth et al., US Patent Nos. 3,540,265 (Nov. 17, 1970); 3,580,058 (May 25, 1971); 3,636,754 (Jan. 25, 1972); *Materials Research and Standards* 10 (8) Cover, 6–11, 40 (Aug. 1970).
[2h] T. G. Sutton, Sr. and W. J. Anderson, Aerospace Fluidics Applications and Circuit Manufacture, Garrett AiResearch Report.
[2i] T. G. Sutton, Sr. and G. L. Frederick, Application of Fluidics to Small Gas Turbine Engine Fuel Controls, presented at Fluid Power Controls and Systems Conf., Madison, WI (May 23–25, 1973).
[2j] W. L. Webb, AFAPL-TR-73-116 (Dec. 1973).
[2k] L. C. Lynnworth et al., pp. 715–732 in ref. 2a; pp. 83–93 in: *Invited Proceedings, IEEE Ultrasonics Symposium* (1970), IEEE Cat. No. 70C69 SU.
[3a] M. H. November, in: ITT-Barton Bulletin MF-1 (1974); *Oil and Gas J.* (Feb. 21, 1972).
[3b] W. E. Abbotts, US Patent No. 3,648,512 (March 14, 1972); *Instrum. Techn.* 19 (7), 66 (July 1972).
[3c] H. M. Roder, NASA SP-3083, Vol. V (1974).
[3d] L. C. Lynnworth, C. A. Carey, and N. E. Pedersen, AEDC TR 74-77 (1974).
[3e] L. C. Lynnworth and E. P. Papadakis, ONR Final Rpt. 384-32)/04-27-72/468 (May 31, 1974), Section 7.14, AD-780 231/7GA.
[3f] L. Filipczynski, Z. Pawlowski, and J. Wehr, Chap. 6, *Ultrasonic Methods of Testing Materials*, Butterworths (1966).
[3g] R. M. Spriggs, *J. Amer. Cer. Soc.* 45 (9), 454 (Sept. 1962).
[3h] R. B. Martin and R. R. Haynes, *J. Amer. Cer. Soc.* 54 (8), 410–411 (Aug. 1971).
[3i] D. P. H. Hasselman, *J. Amer. Cer. Soc.* 45 (9), 452–453 (Sept. 1962).
[3j] R. W. Faas, *Geophys.* 34, 546–553 (Aug. 1969); 36, 615 (June 1971).
[4a] D. I. Crecraft, *J. Sound Vib.* 1 (4), 381–387 (1964); 5 (1), 173–192 (1967).
[4b] N. N. Hsu, *Exptl. Mech.* 14 (5), 169–176 (May 1974).
[4c] P. L. M. Heydemann, *Rev. Sci. Instrum.* 42 (7), 983–986 (July 1971).

[4d] D. E. Van Dyck, *Instrumentation in the Aerospace Industry—Vol. 17*, ISA (1971).
[5a] Bell & Howell, *Pressure Transducer Handbook*, CEC/Instrument Div., Pasadena, CA (1974); *Measurements & Data J.* 8 (5), 92 (Sept.–Oct. 1974).
[6a] E. H. Carnevale *et al.*, NASA CR-789 (June 1967); in NASA SP-132 (June 1967); *J. Chem. Phys.* 46 (8), 3040–3047 (April 15, 1967); 47 (8), 2829–2835 (Oct. 15, 1967).
[6b] K. F. Herzfeld and T. A. Litovitz, *Absorption and Dispersion of Ultrasonic Waves*, Academic Press (1959).
[6c] L. C. Lynnworth *et al.*, *IEEE Trans. Nucl. Sci.* NS-18 (1), 351–362 (Feb. 1971).
[6d] W. P. Mason, *Trans. Amer. Soc. Mech. Eng.* 69, 359–370 (May 1947); *Piezoelectric Crystals and Their Application to Ultrasonics*, pp. 339–350, Van Nostrand (1950).
[6e] W. P. Mason *et al.*, *Phys. Rev.* 75, 936 (1949).
[6f] R. S. Moore and H. J. McSkimin, pp. 170–173, in: W. P. Mason and R. N. Thurston, *Physical Acoustics, Principles and Methods*, Vol. VI (1970).
[6g] E. P. Papadakis, *J. Appl. Phys.* 45 (3), 1218–1222 (March 1974).
[6h] J. D. Richard, US Patent No. 3,194,057 (July 13, 1965).
[6i] P. Macedo and T. A. Litovitz, *Phys. Chem. Glasses* 6 (3), 69 (1965).
[6j] J. H. Simmons and P. Macedo, *J. Acoust. Soc. Amer.* 43 (6), 1295–1301 (June 1968).
[7a] Work of M. S. McDonough, reported in: L. C. Lynnworth, *Materials Eval.* 27 (3), 60–66 (March 1969).
[7b] J. F. W. Bell, Paper J52, *Proc. 4th Intl. Cong. Acoustics*, Copenhagen (1962).
[7c] J. H. Bradshaw, Ph.D. Thesis, Boston College (1972).
[8a] See Ref. 1f, 6c; J. M. Laplant and D. J. Flood, *Cryo.* 12 (3), 234 (June 1972); R. W. Smith, C. K. Day, and W. L. Kelly, 699–702, in: *Proc. IEEE Ultrasonics Symposium (1974)*.
[8b] J. R. Frederick, *Ultrasonic Engineering*, Wiley (1965).
[8c] N. S. Ageeva, *Akusticheskii Zhurnal* 6 (1), 120–121 (Jan.–March 1960).
[9a] E. M. Zacharias, Jr., *Oil & Gas J.* 68 (27), 96 (1970); 70 (Aug. 21, 1972).
[9b] K. A. Fowler and L. C. Lynnworth, *Proc. 6th Int'l. Cong. NDT* (Hannover, Germany) (June 1970).
[9c] See ref. [11c].
[10a] D. R. Hub, Paper J51, *Proc. 4th Intl. Cong. Acoustics*, Copenhagen (1962).
[10b] E. A. Thorne, *ibid*, Paper P23.
[10c] E. P. Papadakis *et al.*, *J. Acoust. Soc. Amer.* 52 (3), Part 2, 850–857 (1972).
[10d] E. P. Papadakis *et al.*, *J. Appl. Phys.* 45 (6), 2409–2420 (March 1974).
[11a] R. C. McMaster, ed., *NDT Handbook*, Vol. II, Sections 43–51, Ronald (1959).
[11b] H. Krautkrämer, *Proc. 4th Intl. Conf. NDT*, 155–158, Butterworths (1964).
[11c] G. V. Jeskey, L. C. Lynnworth, and K. A. Fowler, "An Ultrasonic Transmission Technique for Real Time Monitoring of Steel Solidification", to be published.
[12a] C. K. Day and R. W. Smith, 191–194, *Proc. IEEE Ultrasonics Symp.* (1973).
[13a] R. T. Beyer and S. V. Letcher, *Physical Ultrasonics*, Chap. 6, p. 161 ff., Academic Press (1969).
[13b] F. W. Noble, K. Abel, and P. W. Cook, *Anal. Chem.* 36 (8), 1421–1427 (July 1964).
[13c] Z. Hashim, *J. Appl. Mech.* 29 (1), 143–150 (1962).
[13d] H. W. Grice and D. J. David, *J. Chrom. Sci.* 7, 239–247 (April 1967).
[13e] K. P. Lanneau and R. A. Parnell, US Patent No. 3,557,605 (Jan. 26, 1971).
[13f] E. M. Zacharias, Jr., *Instr. and Control Systems*, 112–113 (Sept. 1970), 43 (9).
[13g] M. F. Feil and E. M. Zacharias, Jr., *Brewers Digest* 46 (11), 76, 78–80 (Nov. 1971).
[13h] E. M. Zacharias, Jr. and R. A. Parnell, Jr., *Food Techn.* (1972), 26 (4), 160–166.
13[i] E. M. Zacharias, Jr. *et al.*, *Modern Plastics* (May 1974, 51 (5), 88–90.
[13j] H. Hagy, *Appl. Optics* 12 (7), 1440–1446 (July 1973).
[13k] H. M. Crawford *et al. Anal. Chem.* (Aug. 1964).
[13l] G. M. Varga, Jr., Esso Tech. Rpt. RK-CR-74-8 (15 Feb. 1974); AD780171.
[13m] G. E. Stungis and S. L. Merker, "Elastic Properties of Reconstituted Tobacco as Determined by Ultrasonic Techniques", presented at 28th Tobacco Chemists Research Conference, Rayleigh, N. C. (Oct. 28–30, 1974), to be submitted for publication in Beiträge Z. Tabakforschung.
[14a] H. J. McSkimin, *J. Appl. Phys.* 24, 988 (1953).
[14b] K. A. Fowler, *Metal Progress* 95 (6), 21 (June 1969).
[14c] A. G. Martin, private communication (1968).
[14d] E. P. Papadakis, *Tappi* 56 (2), 74–77 (Feb. 1973).
[14e] E. P. Papadakis, *J. Acoust. Soc. Amer.* 55 (4), 783–784 (April 1974).
[15a] See R. C. McMaster, Ref. [11a].
[15b] J. and H. Krautkrämer, *Ultrasonic Testing of Materials*, 2nd Ed., Springer-Verlag (1969).
[15c] R. S. Sharpe, ed., *Research Techniques in Nondestructive Testing*, Vol. 1, Academic Press (1970); Vol. 2 (1974).
[15d] R. E. Green, Jr., *Ultrasonic Investigation of Mechanical Properties*, Academic Press (1973).
[15e] J. R. Frederick, *Ultrasonic Engineering*, Wiley (1965).
[15f] Anon. NASA SP-5082, *NDT: Trends and Techniques* (1967).
[15g] A. Vary, NASA SP-3079, *NDE Technique Guide* (1973).
[15h] *Proc. 1st to 7th Int'l Conf. NDT.*
[15i] *Proc. 1st to 9th Symp.* on NDT/NDE sponsored by Southwest Research Inst., San Antonio, Tex. 78284.
[15j] W. J. McGonnagle, ed., *Proc. Symp. Physics and Nondestructive Testing*, Southwest Research Institute (1963).
[15k] *ASNT's Journal, Materials Evaluation; Intl. J. NDT; Brit. J. NDT; Materialprüfung; Sov. J. NDT*, etc.
[16a] O. I. Babikov, *Ultrasonics and Its Industrial Applications*, Consultants Bureau (1960); E. P. Papadakis, *Matls. Eval.* pp. 136–139 (March 1965).
[16b] J. Blitz, *Fundamentals of Ultrasonics*, 2nd ed., Plenum (1967).
[16c] E. P. Papadakis, Chap. 15, pp. 269–328, in: W. P. Mason, ed., *Physical Acoustics, Principles and Methods*, Vol. IV, Part B, Academic Press (1968).
[17a] N. N. Hsu, Ref. [4b].
[17b] J. Krautkrämer, Ref. [11b].
[17c] L. C. Lynnworth, *Ultrasonics* 10 (5), 195–197 (Sept. 1972).
[18a] ASTM STP 505, *Acoustic Emission* (1972).
[18b] J. C. Spanner, *Acoustic Emission—Techniques and Applications*, Intex (1974).
[18c] *Materials Research and Standards* 11 (3), Special Issue on AE (March 1971).
[18d] T. Salzer and C. Martin, U. S. Patent No. 3,794,236 (Feb. 26, 1974).
[18e] R. Higgs, in *Proc. IEEE Ultrasonics Symposium* (1974).
[19a] W. E. Kock, Chap. 5, pp. 297–384 in: W. P. Mason and R. N. Thurston, ed., *Physical Acoustics—Principles and Methods*, Vol. X, Academic Press (1973).
[19b] G. W. Stroke *et al.*, *Ultrasonic Imaging and Holography*, Consultants Bureau (1974).
[19c] R. K. Erf, ed., *Holographic Nondestructive Testing*, Academic Press (1974).
[19d] H. D. Collings, pp. 313–330, in: *Proc. 9th Symp. NDE* (April 1973).
[19e] J. L. Kreuzer and W. R. Arndt, Tech. Rpt., DAAG46-69-C-0010 (Dec. 1970).
[19f] L. R. Dragonette and W. G. Neubauer, *Materials Eval.* 32 (10), 218–222 (Oct. 1974).
[19g] R. Mezrich *et al.*, *Proc. 27th ACEMB Meeting* (Oct. 6, 1974).
[19h] D. Vilkomerson, pp. 283–316, in: P. S. Green, ed., *Acoustical Holography*, Vol. 5, Plenum (1974); see also Vol. 1 (1964), 2 (1970), 3 (1971), 4 (1972).
[19i] P. Greguss, *Physics Today* 27 (10), 42–49 (Oct. 1974).
[19j] B. P. Hildebrand and B. B. Brenden, *An Introduction to Acoustical Holography*, Plenum (1974).
[19k] K. R. Erikson *et al.*, *IEEE Trans. on Sonics and Ultrasonics* SU-21 (3), 144–170, particularly 158–160 (July 1974).
[19l] Acoustic Holography, review in *IEEE Trans. on Sonics and Ultrasonics*, to be published.
[19m] A. Korpel, L. W. Kessler, and P. R. Palermo, *Nature* 232, 110 (1971).
[19n] L. W. Kessler, P. R. Palermo, and A. Korpel, "Practical High Resolution Acoustic Microscopy," *Acoustical Holography*, Vol. 4, Plenum Press, New York (1972), ed. by Glen Wade.
[19o] L. W. Kessler, "Acoustic Microscopy—A New Dimension in Ultrasonic Visualization," in *Proc. Ultrasonics International 1973* (London), IPC Science and Technology Press Ltd. London (1973).
[20a] W. Köster, *Z. f. Metallkunde* 39, 1–9, 9–12 (1948), translated by M. W. Buxton, R&DB, Windscale Works, UKAEA (Sept. 1956).
[20b] M. B. Reynolds, GE Rpt. KAPL-P-881, *Trans. ASM* 45, 839–861 (1953).
[20c] E. H. Carnevale *et al.*, *J. Acoust. Soc. Amer.* 36 (9), 1678–1684 (Sept. 1964).
[20d] L. C. Lynnworth, *Materials Engineering* 68 (6), 8 (Dec. 1968).
[20e] L. C. Lynnworth, J. Testing and Eval. 1 (2), 119–125 (March 1973).
[20f] H. L. Brown and P. E. Armstrong, *Rev. Sci. Instrum.* 34 (6), 636–639 (June 1963).
[20g] R. B. Thompson and G. Alers, pp. 6–19, in *Proc. 9th Symp. on NDE* [15i], (July 1973).

[20h] L. C. Lynnworth, E. P. Papadakis, and W. W. Rea, AMMRC CTR 74-20 (April 1974); pp. 533–536, *Proc. 1973 IEEE Ultrasonics Symposium*, IEEE Cat. No. 73 CHO 807-SU.
[20i] J. Gieske, Sandia Lab. Rep. SAND 75-0043 (Feb. 1975).
[21a] C. P. Albertson and H. E. Van Valkenberg, pp. 147–149, in: *Proc. 4th Int'l. Conf. NDT*, Butterworths (1964).
[21b] See Ref. [6c].
[21c] W. W. Fowlis, *Nature Phys. Sci.* 242, 12–13 (March 5, 1973).
[23] T. T. Anderson *et al.*, pp. 250–269, in [18a].
[24] ——, "Designing Ultrasonic Systems Using PXE Ceramic Air Beam Transducers", Mullard Ltd., Mullard House, Torrington Place, London WC1 E7HD, UK.
[25] J. L. Adams, *Conceptual Blockbusting*, Stanford (1974).

MANUFACTURERS IN NORTH AMERICA

1. Badger Meter, Inc., Controlotron Corp., Datasonics, EDO, EG&G, Endress & Hauser, Inc., Environmental Meas. Systems and Sensor Techn. Co., Jatec, NUSonics, Inc., Ocean Research Equipment Inc., Oceanography International Corp., Panametrics, Parks Elec. Lab., Refac Techn. Development Corp., Saratoga Systems, Inc., Scarpa Labs., Inc., Western Marine Electronics (Wesmar), Westinghouse.
2. Hewlett-Packard, Panametrics.
3. Fluid Data, Inc., ITT-Barton, NUSonics, Panametrics, Solartron/Rockwell Mfg. Co.
4. Hewlett-Packard, Wallace & Tiernan.
5. Columbia, Gulton, Kristal/Kistler, PCB.
6. Bendix.
8. Badger Meter, Inc., Bindicator Co., Bogue Elec. Mfg. Co., Conrac Corp., Controlotron Corp., Datasonics Corp., Delavan Elec. Inc., EG&G, Endress & Hauser, Inc., Industrial Nucleonics Corp., Inventron Industries, Inc., Milltronics Ltd., National Sonics/Envirotech Corp., C. W. Stevens, Inc., Wesmar.
9. NUSonics, Panametrics.
10. Automation Industries, KBI, Magnaflux, Panametrics, Sonic Instrum. Inc.
11. Automation Industries, I.I.I., KBI, Magnaflux, Panametrics, Sloan, Sonic Instrum. Inc.
12. Automation Industries, I.I.I., KBI, Magnaflux, Panametrics, Science Access. Corp., Sloan, Sonic Instrum. Inc., Tempo Instrum. Inc.
13. Baganoff Associates, Inc., DuPont, NUSonics, Tracor.
14. Automation Industries, KBI, Magnaflux, Panametrics, Sonic Instrum. Inc.
15. See Materials Evaluation.
16. Matec.
17. See 10.
18. Acoustic Emission Techn., Dunegan/Endevco, Panametrics, Trodyne Corp.
19. Holosonics, Sonoscope.
20. H. M. Morgan Co., Magnaflux, Panametrics, James Electronics/Instr. Div., Control Products Co., Inc.
22. Delcon/Hewlett-Packard, Dukane Corp./Ultrasonics Div.
23. See 8.
24. See Yellow Pages.
25. See 1–24; Anal. Chem. Lab. Guide; Thomas Register.

Admittance Measurement Accuracies Required to Determine Nonlinear Behavior in Sonar Transducers

JOHN M. HUCKABAY, HOLLIS C. BOEHME, AND ELMER L. HIXSON

***Abstract*—The gain-bandwidth method is an admittance measurement technique which may be used to indicate nonlinear behavior in ferroelectric ceramics. In applying the gain-bandwidth method or a simple plot of admittance versus frequency as practical measures of nonlinearity in ceramic sonar transducers, experimental measurement inaccuracies must be considered. An expression was derived from experimental data to approximate the error associated with frequency determination on an admittance circle plot as a function of admittance measurement accuracy. This expression was included in error analyses which revealed that the expected accuracy with which the gain-bandwidth may be used in determining nonlinear behavior in ceramic transducers is proportional to the admittance measurement accuracy and the mechanical quality factor of the transducer. Results indicate that admittance measurement errors cause extreme difficulty in the detection of nonlinearities in transducers which exhibit low mechanical quality factors typical of high-power sonar systems.**

I. INTRODUCTION

THE NONLINEAR behavior of ferroelectric ceramic material in sonar transducers can seriously degrade the performance of sonar systems at high power levels. Operating a ferroelectric ceramic sonar transducer in its nonlinear region can produce unwanted effects in the acoustic field; these effects are accompanied by a lowering of the electroacoustical energy conversion efficiency. Therefore it is important to determine the drive levels which cause particular transducers to display nonlinear behavior.

Holland and EerNisse describe a procedure which they call the gain-bandwidth method for accurately measuring the properties of a ferroelectric ceramic [1]. Wollett and LeBlanc point out that this method is also a very sensitive indicator of nonlinear conditions in a ceramic [2]. This paper examines the use of the gain-bandwidth method as a practical measurement technique for determining the onset of nonlinear conditions in ceramic sonar transducers.

II. THE GAIN-BANDWIDTH METHOD

When used to determine the onset of nonlinear effects in a ceramic transducer, the gain-bandwidth method requires that complex phasor admittance measurements be recorded as a function of frequency at particular input signal drive levels. The measurements are then plotted to obtain an admittance circle representation of a transducer resonance such as that shown in Fig. 1. From such a representation certain critical points are identified with the

Manuscript received June 24, 1974; revised October 10, 1974. This work was supported by Naval Sea Systems Command, Code 06H, under Contract N00024-74-C-1069, Item 0004.

The authors are with the Applied Research Laboratories, University of Texas at Austin, Austin, Tex. 78712.